Controlled drug delivery systems in eradicating bacterial biofilm-associated infections

Liu, Yong; Li, Yuanfeng; Shi, Linqi

Published in:
Journal of Controlled Release

DOI:
10.1016/j.jconrel.2020.10.038

Publication date:
2021

Journal of Controlled Release 329 (2021) 1102–1116

Contents lists available at ScienceDirect

Journal of Controlled Release

journal homepage: www.elsevier.com/locate/jconrel

Controlled drug delivery systems in eradicating bacterial biofilm-associated infections

Yong Liu [a,b,1], Yuanfeng Li [a,c,1], Linqi Shi [a,*]

[a] State Key Laboratory of Medicinal Chemical Biology, Key Laboratory of Functional Polymer Materials, Ministry of Education, Institute of Polymer Chemistry, College of Chemistry, Nankai University, 94 Weijin Road, Tianjin 300071, PR China
[b] Jiangsu Key Laboratory for Carbon-Based Functional Materials & Devices, Institute of Functional Nano & Soft Materials (FUNSOM), Collaborative Innovation Center of Suzhou Nano Science and Technology, Soochow University, 199 Ren'ai Road, Suzhou 215123, PR China
[c] University of Groningen and University Medical Center Groningen, Department of Biomedical Engineering, Antonius Deusinglaan 1, 9713 AV Groningen, the Netherlands

ARTICLE INFO

Keywords:
Mathematical models
Stimuli-responsiveness
Self-adaptiveness
Surface coating
Electrospun fibers

ABSTRACT

Drug delivery systems (DDS) have extensively progressed over the past decades for eradicating the bacteria embedded in biofilms while minimizing the side effects of antimicrobials on the normal tissues. They possess potential in solving the challenges of intrinsic antimicrobial-resistance and poor penetration of antimicrobials into biofilms. However, the guidelines for developing a controlled DDS for combating bacterial biofilms are limited. In this review, classical mechanisms and mathematical models of DDS were summarized in order to lay the foundation of controlled DDS development. Strategies for building controlled DDS were proposed based on the process of biofilm formation, including surface coatings, fibers, nanoparticles as DDS to prevent biofilm formation and eradicate bacterial biofilm-associated infections. The challenges that still remain in DDS design were discussed and future directions were suggested. We hope this review could give a "road map" to inspire readers and boost the development of the new generation of controlled drug release system for antimicrobial applications.

1. Introduction

Conventional antibiotic treatments are becoming increasingly inefficient in controlling bacterial infections, due mainly to the emergence of antibiotic-resistant pathogens. In 2014, the World Health Organization warned that by 2050, bacterial infections will surpass cancers being the No. 1 killer threatening human health if no effective actions are taken [1]. It is also sobering that the development of bacterial resistance is much faster than the development of new antibiotics [2]. As a result, many large pharmaceutical companies are no longer willing to invest in the research and development of new antibiotics. If things go on like this, we will enter the 'post-antibiotic' era [3], facing the situation of no antibiotics available.

Bacteria living in their biofilm-mode of growth contribute greatly to the emergence of drug-resistance [4–6]. A biofilm is a cluster of bacteria and self-produced extracellular polymeric substances (EPS), such as polysaccharides, extracellular DNA, and proteins [7]. Many factors contribute to the enhanced drug-resistance of biofilms. Firstly, a great part of conventional antibiotics, such as aminoglycosides and polymyxins, possess positive net charge and can interact with the negatively charged extracellular polymeric substances in biofilms, greatly hindering the penetration of antibiotics in biofilms. Secondly, bacteria embedded in biofilms are in their slow-growing phenotype, which is featured by reduced uptake of nutrition, as well as other toxic substances, such as antibiotics. Thirdly, there are a large number of enzymes secreted by the embedded bacteria in biofilms, which could hydrolyze and de-activate the antibiotics. Besides, there are also some other reasons that account for the antibiotic resistance in biofilms as summarized in literature [6]. Taken together, bacterial biofilms are around 10 to 1000 folds more resistant to antibiotics than their planktonic counterparts. What's worse, biofilms account for more than 60% of bacterial infections in humans [5], causing persistent and chronic infections.

To rejuvenate antibiotic treatments and solve the recalcitrance of bacterial biofilms to antimicrobials, both local and systemic controlled

* Corresponding author.
E-mail address: shilinqi@nankai.edu.cn (L. Shi).
[1] These authors contributed equally: Yong Liu, Yuanfeng Li.

https://doi.org/10.1016/j.jconrel.2020.10.038
Received 23 August 2020; Received in revised form 15 October 2020; Accepted 18 October 2020
Available online 22 October 2020

DDS have been developed over the past decades. On one hand, the controlled DDS as surface coating could inhibit the adhesion/growth of bacteria on the surfaces of tissues or implants, reducing the formation of bacterial biofilms (Fig. 1a). On the other hand, the penetration of loaded antimicrobials into biofilms could be enhanced [5], as well as various antimicrobials could be delivered, using multifunctional controlled DDS. Meanwhile, some controlled DDS could smartly target the infected sites and release antimicrobials inside of biofilms [8], efficiently enhancing the bacterial killing efficacy and reducing the potential side effects to normal tissues (Fig. 1b). However, as a drawback, some DDS often show a fast then slow drug release once being administered [9]. This kind of drug delivery system often experiences an undesired leakage of antimicrobials before reaching the infected sites, which could promote the development of antimicrobial-resistance. An ideal drug delivery system for biofilm treatment should maintain the concentration of antimicrobials in blood or tissue around biofilms between minimum effective concentration (MEC) and minimum toxic concentration (MTC) for a certain duration, which will be beneficial in reducing the potential toxicity of drugs and improving patient compliance [10]. However, many factors such as matrixes of the carriers, the interactions between drugs and carriers, and the physicochemical properties of drugs may affect the release rate of DDS [11,12]. Meanwhile, more requirements, such as smart, self-regulated release, and targeted delivery, are in direly need for future antimicrobial applications [9].

In this review, classical mechanisms and mathematical models of DDS were summarized in order to better understand the mechanisms and lay the foundation to develop new DDS. Meanwhile, the recent progress in the design and preparation of controlled DDS were studied to propose strategies for building controlled DDS, including surface coatings as DDS for preventing biofilm formation and eradicate local biofilm infection, and nanoparticles as DDS for systemic infection treatment. The challenges remained in DDS design were discussed and future directions were suggested, in order to give a "road map" to inspire readers and boost the development of the new generation of controlled drug release system for antimicrobial applications, particularly in combating bacterial biofilms.

2. Classical mechanisms and mathematical models of drug delivery system

In the process of the understanding mechanism of drug release behavior from DDS, various theories have been established including diffusion-controlled, swelling-controlled, osmosis-controlled, drug dissolution-controlled, and chemically controlled mechanisms [12,13]. These theories summarized from certain cases promoted DDS from the first generation, such as oral delivery and transdermal delivery, to the second generation (smart DDS) [9].

In general, drug release behavior was affected by multiple complex factors, including characteristics of the delivery system (*e.g.* the composition of matrix, structure, and geometry), release environment (*e.g.* pH, temperature, ionic strength, and enzymes), and properties of the solutes (*e.g.* solubility and interaction with matrix). Among them, there is usually a key factor as the driving force to determine the release rate, called rate-limiting factor. Thus, in most cases, only the rate-limiting factor needs to be considered when describing the drug release rate. Mathematical models not only describe the drug release profiles but also can predict drug release at a specific time point. DDS can be classified by different mechanisms, herein the classical mechanisms and their commonly used mathematical models were discussed, including the drug diffusion-controlled, dissolution-controlled, erosion-controlled, and multicomponent-controlled systems.

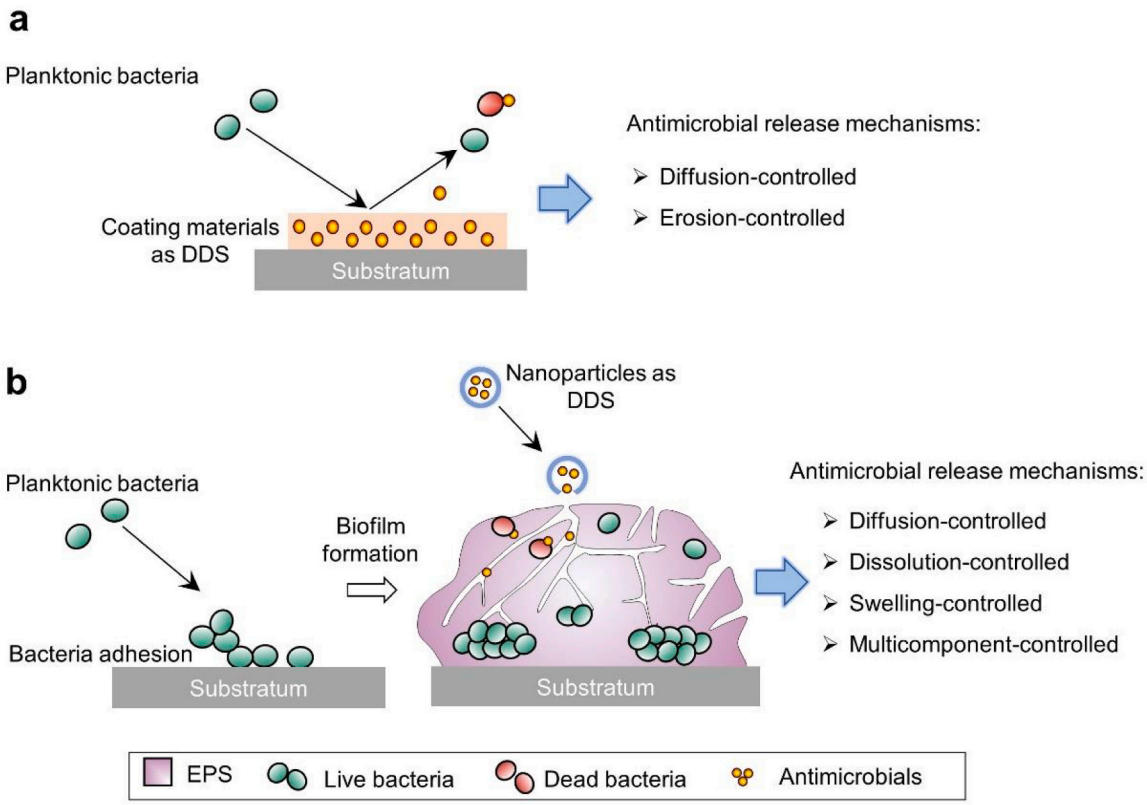

Fig. 1. Illustration of the adhesion of planktonic bacteria to the antimicrobial delivery system modified substratum (a) and unmodified substratum followed by biofilm formation (b). Two kinds of controlled drug delivery systems (DDS) and their probable release mechanisms are demonstrated. Surface coatings as DDS to release antimicrobials for preventing biofilm formation and eradicating local biofilm infection (a) and nanoparticles as DDS to release antimicrobials for systemic infection caused by biofilms (b).

2.1. Diffusion-controlled mechanism

In the diffusion-controlled DDS, drug diffusion is the predominant factor determining the drug release behavior. Fick's law (1) and Fick's second law of diffusion (2) were used as the foundation to quantify diffusion mass transport [14,15].

$$F = -D\frac{\partial C}{\partial X} \tag{1}$$

$$\frac{\partial C}{\partial X} = D\left(\frac{\partial^2 C}{\partial x^2} + \frac{\partial^2 C}{\partial y^2} + \frac{\partial^2 C}{\partial z^2}\right) \tag{2}$$

where F is the rate of transfer per unit area of section (flux), c is the solute concentration, and D is the diffusion coefficient.

The following assumptions were proposed to simplify the release environment and get the simplest cases for the further solution of Eq. (1) and (2): diffusion coefficient of solute is constant, perfect sink conditions are provided in the medium during the entire release period, the swelling and eroding of drug carriers are negligible, and mass transfer resistance is negligible [16].

The diffusion-controlled drug delivery system can be classified into different categories according to the distribution of drugs in the carrier material, initial drug content (concerning solubility of a drug), and geometry, as shown in Fig. 2. In the reservoir system, the drug is surrounded by a matrix and located at the center of a carrier material. For the monolithic system, the drug is homogeneously distributed in the whole carrier. The relation between initial drug concentration (C_i) and drug solubility (C_s) is a decisive factor in developing the mathematical model. The geometry of the carrier also plays a critical role in the release rate, in which slab, sphere, and cylinder were mainly studied geometries. Appropriate mathematical equations were developed for each category of diffusion-controlled DDS as shown in Fig. 2 [16]. Some practical examples were studied and verified the validity of proposed theoretical predictions, such as the release of diltiazem•HCl from three types of spherical drug carriers, theophylline from ethylcellulose loaded films, and diprophylline from matrix tablets [16].

2.2. Dissolution-controlled mechanism

Dissolution-controlled DDS usually refers to DDS where the drug release rate is controlled by the dissolution of a polymeric carrier. Noted that the dissolution of a drug also plays a major role when drug with poor aqueous solubility and/or very low dissolution rate, but it is mainly applicable for the administration of a solid drug [13]. The dissolution of polymeric carrier refers to the process that polymer releases its contents to the surrounding fluid when there is thermodynamically compatible solvent, including two transport processes, solvent diffusion, and chain disentanglement [17]. Several factors affect drug release behavior, such as surrounding fluid, polymer molecular weight, polymer diffusion coefficient, solvent coefficient, and solvent-polymer interaction [18].

Narasimhan and Peppas developed a one-dimensional dissolution-controlled DDS where the drug release is controlled by chain disentanglement in the amorphous, un-crosslinked, linear polymer. This molecular mechanism-based mathematical model can be used to describe transport in a film, slab, disk, or tablet in one direction. A steady-state solution was obtained as shown in Eq. (3) [18].

$$-\frac{(S-R)}{B} - \frac{A}{B^2} ln\left[1 - \frac{B}{A}(S-R)\right] = t \tag{3}$$

In Eq. (3), A and B were defined as:

$$A = D_1\left(\nu_{1,eq} - \nu_1^*\right)\left(\frac{\nu_{1,eq}}{\nu_{1,eq} + \nu_{d,eq}} + \frac{1}{\nu_1^* + \nu_d^*}\right) + D_d\left(\nu_d^* - \nu_{d,eq}\right)\left(\frac{\nu_{d,eq}}{\nu_{1,eq} + \nu_{d,eq}} + \frac{1}{\nu_1^* + \nu_d^*}\right)$$

$$B = \frac{\kappa_d}{\nu_{1,eq} + \nu_{d,eq}}$$

The cumulative release was expressed as:

$$\frac{M_d}{M_{d,\infty}} = \frac{\nu_{d,eq} + \nu_d^*}{2l}\left(\sqrt{2At} + Bt\right)$$

where (S-R) represents the gel thickness, which is the portion of the polymer slab is in the rubbery state during the dissolution state. D_1 and D_d are the solvent and drug diffusion coefficient in polymer, respectively. $\nu_{1,eq}$ and $\nu_{d,eq}$ are the solvent and drug volume fractions, respectively. ν_1^* and ν_d^* are the characteristic concentrations of solvent and drug, respectively. k_d is the disentanglement rate of the polymer chains.

The release of cimetidine hydrochloride and diprophylline from poly (vinyl alcohol)-based systems were studied, demonstrating that the model developed by Narasimhan and Peppas could give an accurate prediction of the experimental data [18].

2.3. Erosion-controlled mechanism

Degradable polymers are useful materials to construct smart DDS. The drug release behavior in these systems is controlled by the degradation of carriers, which strongly depends on the functional groups within DDS. Many functional groups were relevant to this kind of drug carriers, such as poly(cyanoacrylates), poly(anhydrides), poly(ketals), polypeptides, poly(acetals), poly(carbonates), and poly(imino-carbonates). At the same time, the pH and ionic strength of the solvent can significantly affect the degradation of polymers, which further decide the drug release rate [19].

There are two erosion mechanisms for drug carriers formed by degradable polymers, surface erosion, and bulk erosion-controlled DDS. For surface erosion-controlled systems, degradation of polymer is much faster than a solvent intrusion into a carrier, thus the erosion only affects the surface of the carrier. In contrast, solvent intrusion into a carrier is much faster than polymer degradation on the surface for a bulk erosion-controlled system, resulting in the rapid disassembly of the entire carrier [20].

The mathematical model developed by Hopfenberg was frequently used to describe the release behavior of surface erosion-controlled DDS [21], as shown in Eq. (4),

$$\frac{M_t}{M_\infty} = 1 - \left(1 - \frac{k_0 t}{c_0 a}\right)^n \tag{4}$$

where M_t and M_∞ are cumulative of drug release at time t and infinite time, respectively. c_0 is the initial drug concentration in the system, a is the radius of the carrier, n is a "shape factor" that for slab $n = 1$, for cylinder $n = 2$ and sphere $n = 3$.

Another mathematical model of surface erosion for the sphere and cylinder was developed by Cooney [22]. The cylinder was chosen for its special geometry, which a range geometry from flat disks to slender rods can be involved by changing the ratio of L/D (L is the length and D is the diameter of the cylinder respectively). For a cylinder of initial length L_0 and diameter D_0, when L/D approaches zero, it represents a slab; When $L/D < 1$, it represents a disc-like cylinder; when $L/D > 1$, it represents a rod-like cylinder. Drug release rate f was quantified by Eq. (5) Where k is a constant [22].

$$f = \frac{(D_0 - 2kt)^2 + 2(D_0 - 2kt)(L_0 - 2kt)}{D_0^2 + 2D_0 L_0} \tag{5}$$

Based on Eq. (4) and taking radial and axial erosion into account, Katzhendler developed a mathematical model for bulk erosion-controlled DDS [23], as shown in Eq. (6)

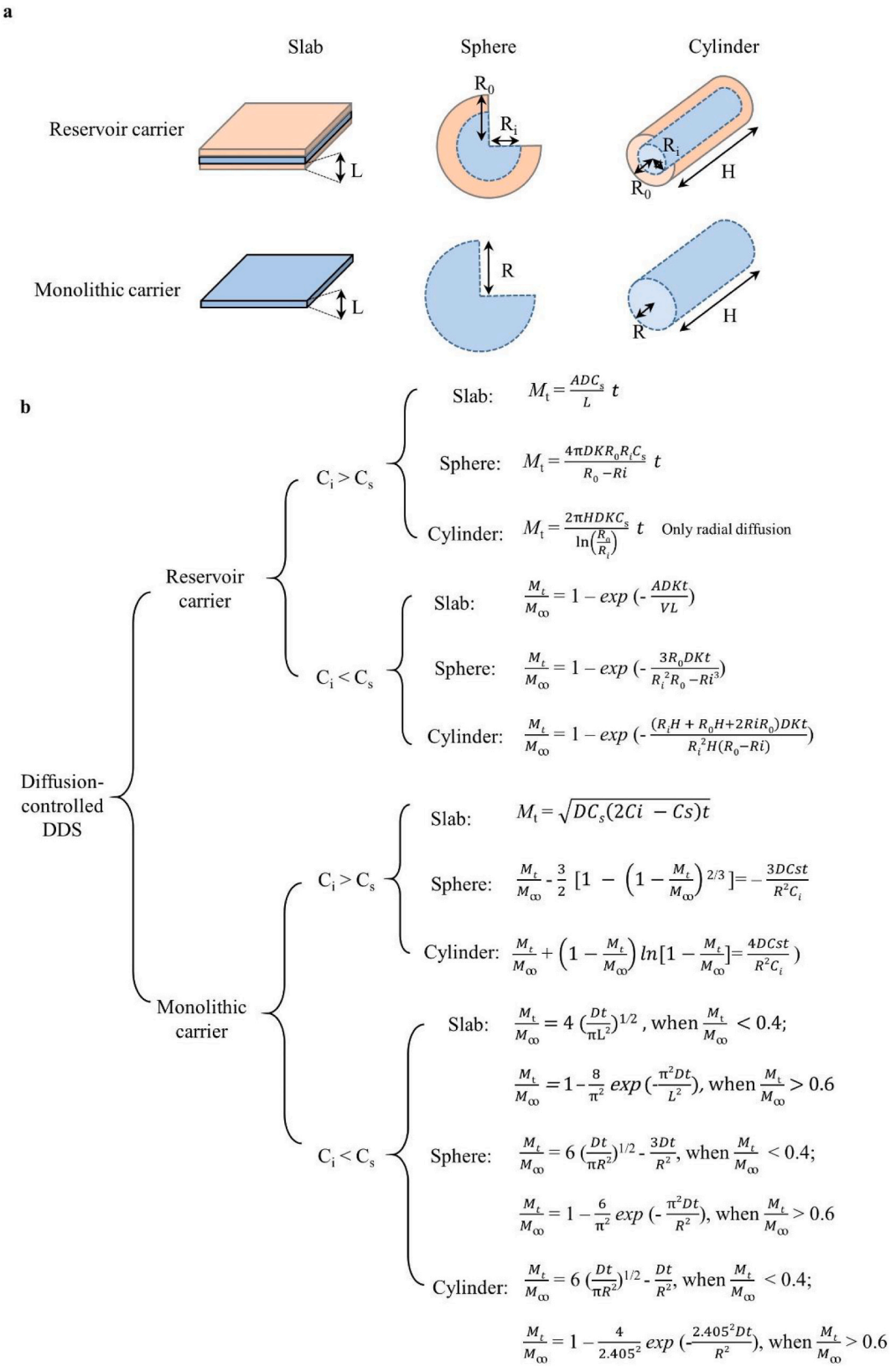

Fig. 2. Classification of diffusion-controlled drug delivery system and their mathematical equations of release behavior. (a) Classification of diffusion-controlled DDS according to geometry, carrier material, and initial drug content. The orange shape indicates the carrier matrix without drug encapsulation, the blue shape indicates drug and carrier matrix are mixed. (b) Mathematical equations of different classified diffusion-controlled DDS. M_t and M_∞ denote the cumulative amounts of drug released at time t and infinity, D is the diffusion coefficient of a drug, V is the volume of the reservoir, A is the surface area of a carrier. (For interpretation of the references to colour in this figure legend, the reader is referred to the web version of this article.)

$$\frac{M_t}{M_\infty} = 1 - \left(1 - \frac{k_a t}{c_0 a_0}\right)^2 \left(1 - \frac{2k_b t}{c_0 b_0}\right) \tag{6}$$

where k_a is the radial erosion rate constant, k_b is the axial erosion rate constant. a_0 and b_0 are the initial radius and thickness of the carrier, respectively.

2.4. Swelling-controlled mechanism

Swelling-controlled DDS are usually composed of hydrophilic polymers. There are two states in the swelling-controlled polymeric carriers, namely the non-swollen state and the swollen state. In the non-swollen state, the polymer network is dense and the mobility of the macromolecules is restricted, upon contact with the solvent, the polymers "relax" to a swollen state, which results in the significantly increased mobility of macromolecules and volume of the carrier system. The drug release behavior is controlled by the change of the physical state of the polymer [24].

Nicholas Peppas developed a power-law approximation to quantify a type of "purely swelling"-controlled drug delivery system, as shown in Eq. (7) [16].

$$\frac{M_t}{M_\infty} = kt^n \tag{7}$$

where M_t and M_∞ are cumulative of drug release at time t and infinite time, respectively. k is a rate constant. n is a geometry factor, for a thin film with negligible edge effects, $n = 1$; for a cylinder, $n = 0.89$; for a sphere, $n = 0.85$.

2.5. Multicomponent-controlled mechanism

For many DDS, their release kinetics were controlled by not only one factor, and often even more processes are simultaneously involved in controlling drug release.

Peppas developed a model for drug carriers made of neat poly (ε-caprolactone) (PCL), neat poly (lactide-*co*-glycolide) (PLGA) and their blends. For neat PCL, two factors were involved in this model: initial burst (first part of Eq.(8)) and followed diffusion-controlled release (the second part of Eq. (8)), and the drug release can be described as shown in Eq. (8). For neat PLGA, three factors were involved: burst release (first part of Eq. (9)), relaxation-controlled release (the second part of Eq. (9)), and diffusion-controlled release (the third part of Eq. (9)). For blend PCL/PLGA, the release from PCL or PLGA in blend follows the same mechanism of its respective unblended state, thus the overall drug release of the blend is a summation of drug release from the PCL phase and PLGA phase, as shown in Eq. (10) [25].

$$\left(\frac{M_t}{M_\infty}\right)_{PCL} = \phi_{b,PCL}\left\{1 - exp\left(-k_{b,PCL}t\right)\right\} + \phi_{d,PCL}\left\{1 - \sum_{n=0}^{\infty} \frac{8}{(2n+1)^2\pi^2} exp\left(\frac{-D_{PCL}\,(2n+1)^2\pi^2\left(t - t_{b,PCL}\right)}{4l^2}\right)\right\} \tag{8}$$

$$\left(\frac{M_t}{M_\infty}\right)_{PLGA} = \phi_{b,PLGA}\left\{1 - exp\left(-k_{b,PLGA}t\right)\right\} + \phi_{r,PLGA}\left\{exp\left[k_{b,PLGA}t\right] - 1\right\} + \phi_{d,PCL}\left\{1 - \sum_{n=0}^{\infty} \frac{8}{(2n+1)^2\pi^2} exp\left(\frac{-D_{PLGA}\,(2n+1)^2\pi^2\left(t - t_{b,PLGA}\right)}{4l^2}\right)\right\} \tag{9}$$

$$\left(\frac{M_t}{M_\infty}\right)_{blend} = f_{PCL}\left(\frac{M_t}{M_\infty}\right)_{PCL} + f_{PLGA}\left(\frac{M_t}{M_\infty}\right)_{PLGA} \tag{10}$$

where M_t and M_∞ are the cumulative of drug release at time t and infinite time respectively. ϕ_b and ϕ_d are the fractions of drug release through burst phase and diffusion respectively (same for PCL and PLGA), noted that $(\phi_b + \phi_d) = 1$. f_{PCL} and f_{PLGA} are the fractions of drug that partition into and are released from PCL and PLGA phases respectively, noted that $f_{PCL} + f_{PLGA} = 1$.

Paclitaxel was loaded into neat PCL, neat PLGA and a blend of PCL/PLGA to study the release behavior. The applicability of the developed model has been tested and proven effective on a range of different PLGA and PCL ratios in the blend [25].

Siepmann and Peppas developed a model that simultaneously considered the diffusion of water and drug with time- and position-dependent diffusivities, moving boundary conditions, the polymer swelling, polymer, and drug dissolution, as well as radial and axial mass transfer within cylindrical tablets [26].

Water and drug diffusion are considered to follow Fick's second law of diffusion, as shown in Eq. (11). C_k and D_k are the concentration and diffusion coefficient of the diffusing item respectively ($k = 1$ for water, $k = 2$ for the drug), r is the radial coordinate of a cylindrical tablet, z is the axial coordinate of a cylindrical tablet, θ is the angular coordinate of a cylindrical tablet [26].

$$\frac{\partial C_k}{\partial t} = \frac{1}{r}\left\{\frac{\partial}{\partial r}\left(rD_k\frac{\partial C_k}{\partial r}\right) + \frac{\partial}{\partial \theta}\left(\frac{D_k}{r}\frac{\partial C_k}{\partial \theta}\right) + \frac{\partial}{\partial z}\left(rD_k\frac{\partial C_k}{\partial z}\right)\right\} \tag{11}$$

According to the free volume theory of diffusion, an exponential dependence of the diffusion coefficients on the water content of the system is taken into account, as shown in Eq. (12) Where, β is a dimensionless constant characterizing this concentration-dependence. D_{eq} represents the diffusion coefficient in the equilibrium swollen state of the system [26].

$$D_k = D_{k,eq}\, exp\left\{-\beta_k\left(1 - \frac{C_1}{C_{k,eq}}\right)\right\} \tag{12}$$

Polymer dissolution is taken into consideration by using a dissolution rate constant k_{diss}, which represents the polymer mass loss velocity normalized to the actual surface area of the system. M_{pt} and M_{p0} are the dry polymer matrix mass at time t and $t = 0$, respectively; A_t denotes the surface area of the device at time t.

$$M_{pt} = M_{p0} - k_{diss}A_t t \tag{13}$$

Ideal mixing is assumed (no volume contraction upon mixing drug, polymer, and water), and the total volume of the system at any instant is given by the sum of the volumes of the single components [26].

The release of propranolol•HCl from cylindrical hydroxypropyl methylcellulose matrices was studied. The agreement between the prediction by the above model and experiment was rather good [26].

3. Surface coatings

Despite the strict sterilization and aseptic procedures during surgeries, many local infections such as implant-associated and peritoneal infections are still inevitable. In principle, biofilm infections are caused by bacterial adhesion to a substratum surface, and certain attached bacterial strains are capable of forming a biofilm [27]. The most direct preventive strategy for biofilm infections is to interfere with bacteria adhesion *via* modifying the micro- and nano-topology of the surfaces of implants or other medical devices [28]. Surface modification using surfactants or dense hydrophilic polymer brushes could generate anti-fouling surfaces that resistant to bacterial adhesion. Moreover, considerable intrinsically antimicrobial implants containing quaternary ammonium-modified surfaces are capable of killing the microbes that are attached [29,30]. Since these surface modification strategies have been well-reviewed in literature [31–33], they are not the subjects of this section. Here, strategies for surface coating were summarized based on their release behavior (Fig. 3), and recently developed surface

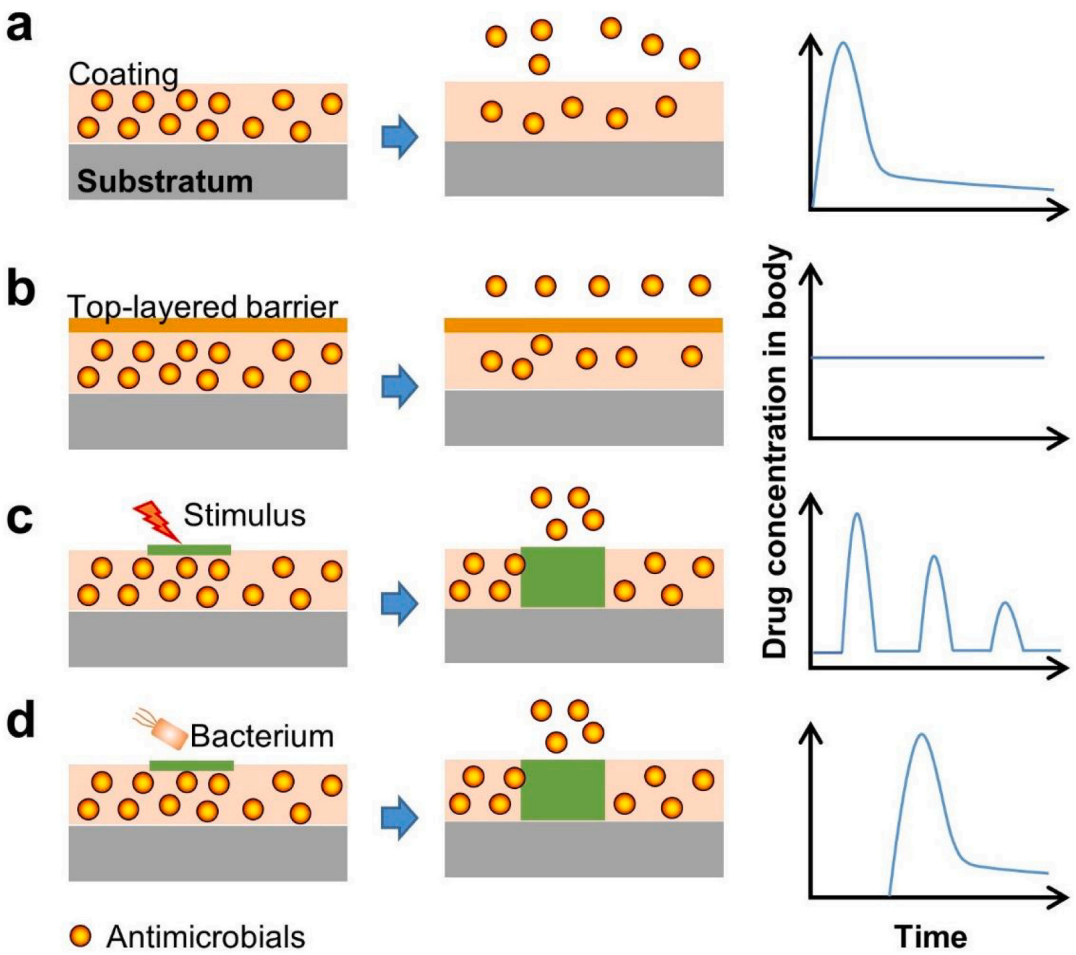

Fig. 3. The design strategies for the antimicrobial-releasing surfaces to control the release of antibacterial agents over space and time. (a) Passive approaches and rapid burst release from the antimicrobial coatings. (b) Controlled approaches and the linear release from the antimicrobial coatings. (c) Active approaches and the triggered local release of embedded compounds. (d) Bacteria-triggered approaches and bacteria-responsive coatings release antibacterial agents locally when challenged by bacteria.

coatings that loaded antibiotics, antimicrobial peptides, nitric oxide, metal ion as antimicrobials were summarized, as well as a special triggered-release coating surface.

3.1. *Antibiotic-releasing surfaces*

Commonly used strategies to prevent implant-associated infections are local delivery systems of antibiotics, in which antibiotics could be released in a controlled manner for hours to months [34–36]. During that period, the released antibiotics are capable of eradicating the surrounding pathogens without provoking the drug-resistance. In general, antibiotics could be immobilized on the surfaces of implants *via* either covalent or non-covalent methods.

Many antibiotics, such as vancomycin, daptomycin, gentamicin, ceftriaxone, and kanamycin, have been reported to be tethered onto the surfaces of titanium, glass, quartz, gold, silicone, and silica [34] *via* chemical bonds like amides. For this purpose, the surface of implants needs to be functionalized first. For instance, pure titanium needs to be oxidized with chromic acid or piranha acid or treated *via* hydrothermal aging. Subsequently, chemical agents, in particular, amino-propyltriethoxy silane (APTES), are applied to treat the aforementioned surfaces, yielding the surfaces with flanking amines that could further conjugate with antibiotics. Of note, the majority of these antibiotics conjugated on the implant surfaces are not cleavable. Therefore, these systems can prevent the attachment of bacteria and the formation of their biofilms yet, not effective in eradicating the bacteria floating in interstitial fluid. Whereas, the antibiotics conjugated onto the surfaces of implants *via* the hydrolyzable chemical bonds, such as esters [35] and anhydrides [36], could be released in the presence of certain bacterial enzymes.

Most of the antimicrobial implant coatings are constructed *via* dip coating of polymers such as poly(lactic-*co*-glycolic acid) (PLGA), PCL, hydroxyapatite, polyurethane (PU), and collagen, as well as directly incorporate antibiotics to form the antibiotic-releasing surfaces. To this end, it was quite difficult to tune the corresponding drug loading content, dosage, or release rate [27,37].

For controllable antibiotics release, layer-by-layer (LbL) is the most commonly used strategy [38–40]. In general, there are several approaches to incorporate antibiotics into the LbL system. Firstly, the charged antibiotics, such as gentamicin, could be directly used as part of the coated layers to be deposited onto the surfaces. For instance, in the pioneering work by Hammond and co-workers, polyelectrolyte multilayers were fabricated using the positively charged poly(β-amino ester) (PBAE) [41], gentamicin, and polyanionic hyaluronic acid (HA) [38]. Encapsulation dosage ranging from 0 to ~150 μg/cm^2 could be easily adjusted by changing the number of deposited layers and the PBAE used. Also, the release rate of the loaded antibiotics could be adjusted by polymer chemistry and film architectures. For instance, LbL films built from the repeat {PBAE/polyacrylic acid (PAA)/gentamicin/PAA} exhibited a burst release of gentamicin from the surface at a rate of 11 μg/cm^2/day in the first few days, followed by sustained release of 4 μg/cm^2/day over serval weeks [39]. This is possibly due to freely absorbed

gentamicin molecules on the top layers of the films, yielding a combination release profiles of rapid out-diffusion and slow hydrolytic degradation of the deeper {PBAE/PAA/gentamicin/PAA} layers. Similarly, vancomycin [42] was encapsulated in the LbL films for the sustained release of antibiotics to control the formation of biofilms. Besides, uncharged antibiotics could be conjugated to one of the polyelectrolytes [43] and loaded into the LbL films.

3.2. Antimicrobial peptides-releasing surfaces

Antimicrobial peptides usually carry positively charged segments. Therefore, antimicrobial peptides could be used as building blocks to construct the LbL films that decorate the surfaces of implants. For instance, seventy-five tetralayer (PBAE/polyanions/ponericin G1/polyanions) films were deposited, where polyanions (*e.g.* alginic acid, chondroitin sulfate, dextran sulfate) were employed [44]. The films composed of chondroitin sulfate and alginic acid exhibited similar release profiles, where a burst release of 62% and 65% of the total loaded antimicrobial peptide in the first 24 h, for chondroitin sulfate and alginic acid films, respectively. Whereas, films derived from dextran sulfate exhibited a linear release profile, especially in the first several days. Moreover, all the films achieved sustained release up to 10 days, thereby inhibiting the *Staphylococcus aureus* (*S. aureus*) attachment and biofilm formation. Although antimicrobial peptides possess the advantages such as being compatible, degradable, and less likely to provoke the drug resistance, these peptides are usually quite sensitive to proteases and of low cost-effectiveness, limiting their further application and clinical translation.

3.3. Nitric oxide (NO)-releasing surfaces

To overcome the antibiotics resistance crisis, nitric oxide (NO) has been regarded as an excellent candidate. NO is of low antimicrobial efficacy itself. However, NO can react with oxygen and other reactive oxygen species such as superoxide (O^{2-}) to generate more lethal species that can damage the lipids and biomacromolecules of bacteria [45]. Particularly, NO has been demonstrated to exhibit both bactericidal and biofilm-dispersal activities [46,47]. Since NO is a gas therapeutic and has a very short life-time of only several seconds, which greatly limited its biological application. To solve this dilemma, numerous NO donors such as metal–NO complexes, organic nitrates, *N*-diazeniumdiolates, and *S*-nitrosothiols have been developed. However, these donors decompose spontaneously when they are dissolved in an aqueous solution. Fortunately, the half-lives of these donors could be prolonged from seconds to hours by designing the structure of the amine precursor [48]. To achieve continuous NO release to prevent biofilm formation, NO-releasing surfaces have been prepared. For example, dibutyhexyldiamine diazeniumdiolate (DBHD/N_2O_2) was deposited in a PLGA layer and further encapsulated in a silicone rubber top coating to form the NO-releasing films. The PLGA layers could control the release of DBHD/N_2O_2 by its intrinsic acid residues and hydrolysis products. The optimized films achieved a controlled NO release for one week. Besides, these NO-releasing films exhibited considerable antibiofilm properties against both *S. aureus* and *Escherichia coli* (*E. coli*), reducing more than 98% of the biomass in those biofilms [49]. Similarly, *S*-nitroso-*N*-acetylpenicillamine and polyurethane (PU) were doped to form the S-Nitroso-*N*-acetylpenicillamine (SNAP)-textured PU films, which exhibited a lifetime of up to 10 days at flux levels above 0.5×10^{-10} mol min^{-1} cm^{-2} and inhibited the *Staphylococcus epidermidis* (*S. epidermidis*) biofilm formation for >28 d [50]. Besides, block polymer such as poly (ethylene glycol)-*block*-polycaprolactone (PEG-*b*-PCL) was also used to top-coat the NO-donor layer. Of note, the PEG-*b*-PCL top-coated films exhibited prolonged and well-controlled NO-release profiles, outperforming the PEG or PCL coated films [51].

Besides, NO-donor could be covalently immobilized on surfaces to inhibit the growth of bacterial biofilms. For example, SNAP was immobilized to poly(dimethylsiloxane) (PDMS) layer, yielding a highly stable NO-releasing material that inhibited bacterial biofilm formation for over 125 days [51]. Similarly, the NO donor *N*-diazeniumdiolates were formed *via* the reaction of NO gas with polydopamine (PDA) layer, and NO release from this PDA coating was observed for 2 days [52].

3.4. Metal ion-releasing surfaces

Metal ions have been applied for infection control for thousands of years. Metal ions possess multiple antimicrobial mechanisms including but not limited to inducing the generation of reactive oxygen species, inhibiting enzymatic activity, and depleting antioxidants [5,53,54]. Free ions were commonly incorporated into surfaces *via* the coordination bonds. Therefore, the release rate of these free metal ions is considerably difficult to control [55,56]. Recent strategies have been focused on the construction of metal nanoparticles and polymer composite coatings [57]. Metal ions are frequently released from the surfaces of their corresponding nanoparticles due to the high surface to volume ratios of nanoparticles [54,57]. To this end, numerous metal nanoparticles such as silver [58–60], titanium [61], zinc [37,62], gold [63,64], and palladium [65,66] nanoparticles have been constructed to the surfaces of titanium and stainless steel with the assistance of polymers. Although most of these metal nanoparticle-embedded coatings could prevent the initial attachment of bacteria and the subsequent formation of biofilms *in vitro* over several months [60], their biological application is largely limited by the potential concentration-dependent cytotoxicity of metal ions, especially silver ions, to the normal mammalian cells and emergence of drug-resistance strains.

3.5. Triggered-release surfaces

Polymers and polymer-based hydrogels can undergo volume variations (swelling, bending, or shrinking), structural transformations, or even chemical bond cleavage upon the trigger of various stimuli, leading to the efflux of the loaded antimicrobials from the matrix. Both external and internal stimuli have been applied to design the triggered-release surfaces, generating 'on-demand' antibacterial effects and extending the lifetime of coatings [53,67]. Light [68], ultrasound [69,70], electrical [71–73], magnetic fields [74] sensitive coatings/hydrogels have been developed for bacterial biofilm-associated infection control. Whereas, the main challenges facing stimuli-triggered coatings are to maintain the release of antimicrobials with effective doses over multiple cycles and to minimize non-triggered antimicrobial leakage from surfaces.

Besides, bacterial infections are closely associated with physiological factors such as low pH and over-expressed enzymes. These factors are of great importance because they greatly implicate antimicrobial treatments [75] and can be used to design the bacteria-triggered release surfaces. For example, the LbL films formed by tannic acid and various cationic antibiotics (tobramycin, gentamicin, and polymyxin B) were found to be responsive to the acidic microenvironment produced by pathogenic bacteria, releasing the loaded antibiotics in a 'self-defensive' manner [76]. A similar 'self-defensive' strategy has been used to construct bacterial enzyme-responsive coatings [43,77]. For example, cateslytin (CTL) was chemically conjugated to hyaluronic acid (HA), which was deposited on a planar surface with positively charged chitosan (CHI) to form the (HA-CTL-C/CHI) films [43]. The resulting HA-CTL-C/CHI films completely inhibited the development of *S. aureus* and *Candida albicans* (*C. albicans*) biofilms.

4. Electrospun fibers

Electrospinning is a popular fiber manufacturing technique in which a strong electrical potential is utilized to draw and solidify polymer-containing solutions or melts, yielding microscale or nanoscale fibers [78]. This technique allows for the spinning of both natural polymers

and synthetic polymers, incorporating both hydrophobic and hydrophilic antimicrobials into the fibers [79] with diameters ranging from 100 nm to several microns. Electrospun fibers could be used as 1D bundles/yarns, 2D membranes/films, or 3D scaffolds [80], potentiating their applications in large scale antimicrobial DDS preparation and application.

Typically, a setup for electrospinning contains three basic parts: a high voltage power supplier, a spinneret, and a grounded collector, as shown in Fig. 4. Since the recent developments in electrospinning technologies have been extensively discussed in many reviews [81–83], the subjects of this section are the electrospinning technologies to facilitate the antimicrobial loading and release, as well as their biological applications, especially in building antimicrobial surface. In general, technologies such as uniaxial electrospinning, coaxial electrospinning, triaxial electrospinning, and multifluidic electrospinning have been used to prepare the antibiotics-containing fibers by choosing different spinnerets, as illustrated in Fig. 4. Uniaxial electrospinning employs a mixed solution of a polymer and functional component to generate monolithic fibers. Coaxial electrospinning uses two-fluid side-by-side. Triaxial electrospinning can be carried out to generate nanofibers using three (outer, middle, and inner) same liquid as working solutions. As a result, the uniaxial fibers possess uniform structures. Whereas, the coaxial fibers possess core-sheath structures, and the triaxial fibers possess core-intermediate layer-sheath structures (Fig. 4d–f).

The antimicrobial release from electrospun fibers largely depends on the structures of electrospun fibers. Drug-loaded uniaxial fibers tend to exhibit an uncontrollable initial burst of release. This arises for three reasons: (1) the presence of large numbers of drug molecules at or near the surface of the fibers; (2) the large surface area and high porosity of the fiber mats; and (3) the fact that drug molecules in the center of the fibers have to diffuse further to reach the bulk solution during the dissolution process than those at the surface [86]. For example, the mefoxin-loaded PLGA fibers and tetracycline-loaded polyvinyl alcohol (PVA)/Chitosan fibers exhibited a burst release of their cargoes in the first several hours [87,88]. As we summarized in Table 1, most of the antimicrobial-loaded uniaxial fibers exhibited the fast-then-slow biphasic release profiles, with a subsequent antimicrobial release up to several weeks.

Recently, coaxial and triaxial electrospinning technologies have been developed and extensively used in drug delivery. The advanced electrospinning approach allows for precisely tuning drug release from nanoscale formulations. Normally, the coaxial and triaxial fibers can achieve better-controlled drug release profiles compared to the uniaxial fibers. Especially, triaxial electrospinning is possible to produce drug-loaded fibers coated with a thin polymer shell layer by using two unspinnable and a spinnable liquid as the outer, middle, and core working fluids. The resulting core-shell nanofibers gave close to zero-order drug release over periods which could be tuned simply by adjusting the thicknesses of the shell [86]. Whereas, this technology is still in its infancy and has not been widely used for the delivery of antimicrobials.

As mentioned above, the electrospun fibers can be formulated in 1D, 2D, and 3D materials, which enable their applications as wound dressing patches or other tissue engineering matrixes [101,102]. Therefore, most of the recent studies have been restricted to pathogenic strains such as Gram-positive bacteria (*S. aureus*, *S. epidermidis*) and Gram-negative bacteria (*E. coli*, *P. aeruginosa*). Some conventional antibiotics with a broad-spectrum bactericidal ability such as tetracycline [88,93,96], ciprofloxacin [94,101], and ampicillin [98] have been loaded into electrospun fibers. Other antimicrobials such as chlorhexidine [95] have also been employed in fabricating antimicrobial fibers. However, the use of antibiotics or antimicrobials may cause the emergence of bacterial antimicrobial resistance. To solve this problem, several antimicrobial proteins have also been employed in fabricating the antimicrobial electrospun fibers. For example, zein, lysostaphin, and nisin were loaded

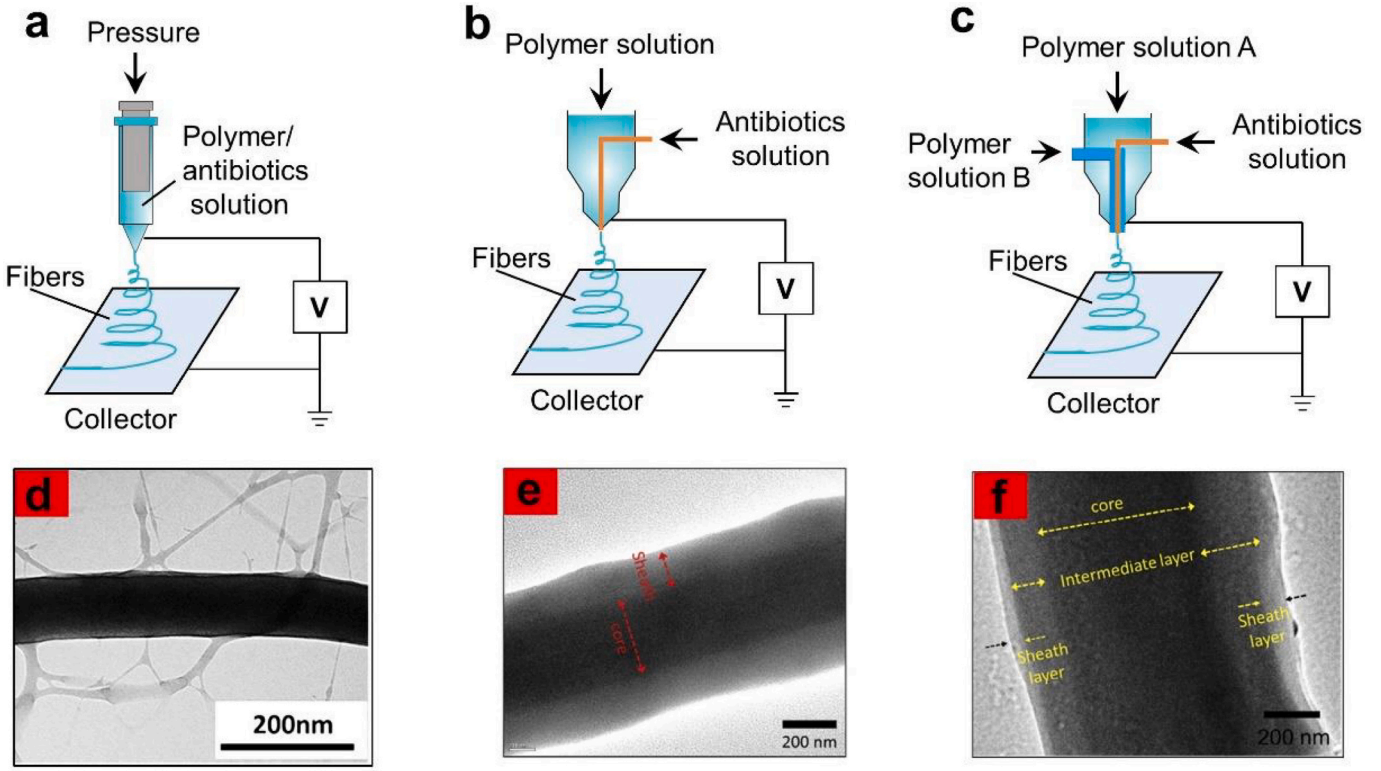

Fig. 4. Schematic illustration of the setup for (a) uniaxial electrospinning, (b) coaxial electrospinning, and (c) multifluidic electrospinning with multiple spinnerets. Exemplary TEM images showing the structures of (d) uniaxial fibers, (e) coaxial fibers, and (f) triaxial fibers. Panel d reprinted with permission from Ref. [84]. Copyright (2018), Elsevier Ltd. Panels e and f reprinted with permission from Ref. [85]. Copyright (2017), Elsevier Ltd.

Table 1
Summary of the recent development of electrospun fibers for antimicrobial application.

Polymers	Antimicrobials	Loading wt%	Fiber diameter (nm)	Release profiles	Target strains	Ref.
Uniaxial						
PLGA	Mefoxin	5	700	Burst release, up to 1-week	*S. aureus*	[87]
PVA/Chitosan	Tetracycline	–	110–310	Burst release in the first 3 h	*E. coli* *S. epidermidis* *S. aureus*	[88]
PLGA	Graphene oxide−Silver	–	356	Burst release, up to 4-d	*E. coli* *P. aeruginosa*	[89]
Chitosan	Zein	10	192	–	*S. aureus*	[90]
Cellulose	Lysostaphin	3	450	–	*S. aureus*	[91]
PLGA	Metronidazole	0.1–40	600–1200	Cumulative release up to 7-d	*F. nucleatum, A. actinomycetemcomitans, and P. gingivalis*	[92]
Halloysite nanotubes/PLGA	Tetracycline	1–2	300–600	Sustained-release up to 42-d	*S. aureus*	[93]
PLGA/ poly(dioxanone) (PDO)	Ciprofloxacin	–	–	Sustained-release up to 7-d	*S. aureus* *E. coli*	[94]
Gelatin Cross-linked	Chlorhexidine	0.5–25	4700	Sustained-release at pH 7 and burst release at pH 2	*E. coli* *S. epidermidis*	[95]
PCL	Tetracycline/whey proteins	–	100–500	Sustained release up to 14-d	*E. coli* *S. typhimurium*	[96]
PCL/gelatin	(6-Aminopenicillanic acid, APA)-coated Au NPs	–	~200	Sustained-release up to 14-d	*MDR E. coli* *K. pneumoniae*	[97]
Reduced graphene oxide (rGO)/poly (acrylic acid) (PAA)	Ampicillin or cefepime	–	~400	NIR light-triggered release	*E. coli* *S. aureus* *S. epidermidis*	[98]
Coaxial						
Poly(lactic acid)/chitosan (core/shell)	Chitosan	4	100–1500	–	*E. coli*	[99]
PCL/chitosan	Ag NPs	4–10	100–750	–	*E. coli* *S. aureus*	[100]
Polyvinylpyrrolidone (PVP)/ ethyl cellulose (EC) polymer Janus fibers	Ciprofloxacin (CIP) and Ag NPs	–	600–1000	>90% of CIP was released within the first 30 min	*E. coli* *S. aureus*	[101]
Triaxial						
PCL intermediate/ cellulose acetate sheath	Nisin	1–8.6	–	–	*S. aureus*	[85]

Abbreviations: *Fusobacterium nucleatum* (*F. nucleatum*), *Aggregatibacter actinomycetemcomitans* (*A. actinomycetemcomitans*), *Porphyromonas gingivalis* (*P. gingivalis*), *Salmonella typhimurium* (*S. typhimurium*), *Klebsiella pneumoniae* (*K. pneumoniae*).

into the chitosan and cellulose electrospun fibers [85,90,91], respectively, to combat the *S. aureus*. Also, metal nanoparticles, such as Au and Ag nanoparticles [97,100], have been encapsulated into polymeric electrospun fibers, which demonstrated excellent antimicrobial ability. Some novel antimicrobial materials such as graphene oxide can damage bacterial cell membranes *via* its special lipid extraction mechanism [5] and be compatible with electrospinning technology [89]. Of note, a combination of two antimicrobial agents has also been applied to enhance the antimicrobial ability and minimize the emergence of antimicrobial resistance. For instance, PLGA−chitosan mats functionalized with graphene oxide and silver nanoparticles (GO−Ag) exhibited excellent bactericidal effect against both Gram-negative and -positive bacteria [89].

To achieve stimuli-triggered antimicrobial release from the electrospun fibers, several systems have been developed. For example, glutaraldehyde (GTA) was used to cross-linked the gelatin electrospun mats, yielding the pH-responsive, tunable drug release property [89]. Moreover, reduced graphene oxide (rGO) was embedded poly(acrylic acid) (PAA) fiber mats, where rGO exhibited photothermal property upon NIR irradiation at 980 nm. This local heat produced by rGO upon light irradiation triggered the pulse release of antibiotics ampicillin or cefepime to inhibit the growth of planktonic *E. coli* K12 and *S. epidermis* [98]. Of note, all these antimicrobial electrospun fibers were used to inhibit the growth of bacteria in their planktonic mode of growth. Therefore, their study on eradicating bacteria in their biofilm-mode of growth is highly desired.

5. Nanoparticles

5.1. Biological barriers

To access the systemic infection, the antimicrobial-delivery systems need to overcome several biological barriers. Firstly, the delivery systems are requested to be stable enough when they are injected into the blood and minimize the absorption of opsonin proteins to avoid the recognition and clearance of immune cells. Moreover, it has been reported that nanoparticles with a size smaller than 5 nm are prone to be cleared *via* renal filtration [103]. Whereas, particles bigger than 500 nm are easy to recognize by the reticuloendothelial system (RES) [104]. Therefore, particles ranging from 5 nm to 500 nm might be suitable for antimicrobial delivery [5,105]. Moreover, in inflammatory conditions induced by microbe infection, the pathogens may secrete factors that increase the permeability of blood vessels [106]. Therefore, the nanoparticles with diameters less than 200 nm could passively accumulate at the infected sites due to the enhanced permeability and retention (EPR) effect [107], similar to that found in tumor sites [108]. Upon reaching the sites of infection, the antimicrobial-loaded delivery systems need to penetrate the extracellular polymeric substances of biofilms efficiently and bind to the embedded bacterial cells. The loaded antimicrobials should be released inside biofilms to exert their bactericidal efficacy. The use of nanotechnology to overcome the biological barriers of treating systemic infections has been well-summarized in literature [109–113]. Here we summarized the main strategies for designing

antimicrobial-releasing nanoparticles, based on their different release mechanisms and release behaviors (Fig. 5).

5.2. Diffusion-controlled systems

Unlike the local delivery systems that can release their cargoes for a long period, the nanoparticles administered systemically usually have a short half-life of only a few minutes to a few hours. Therefore, the time window for drug release from their carriers is quite short. Besides, the local concentration of antimicrobial is requested to higher than the minimal inhibition concentration of that specific strain in order to achieve a satisfactory bactericidal effect. To this end, a fast release of the loaded antimicrobials at an infected site is highly desired.

Nanoparticles such as liposomes, micelles, mesoporous silica nanoparticles, dendrimers, metal nanoparticles have been investigated for eradicating bacterial biofilms [114,115]. Hydrophilic antimicrobials such as most of the conventional antibiotics and antimicrobial peptides can be encapsulated in the aqueous cores of liposomes [116] or the aqueous channels of silica nanoparticles [117]. Whereas, hydrophobic antimicrobials can be loaded in the hydrophobic cores of micelles [8] or shells of liposomes [116]. The interactions of antimicrobials with their carriers are usually non-covalent bondings such as hydrophobic, π-π stacking interactions, electrostatic attractions, and coordination bonding [5]. In general, these weak interactions allow the fast diffusion of antimicrobials when the nanocarriers reach their targets. Particularly, liposomes composed of the lipid bilayer can undergo lipid fusion [118] with bacterial cell membranes and release the loaded antimicrobials directly into the bacterial cells [119]. Therefore, these systems usually possess considerably efficient bactericidal efficacy. One major drawback of these free diffusion systems is that they start to release the loaded antimicrobials once they are suspended in aqueous solutions (Fig. 5a), causing premature drug leakage and potential side effects. For example, we loaded the hydrophobic antimicrobial triclosan into mixed-shell polymeric micelles (MSPMs) that composed of poly(ethylene glycol)-*block*-poly(ε-caprolactone) (PEG-*b*-PCL) and poly(β-amino ester)-*block*-poly(ε-caprolactone) (PAE-*b*-PCL). The formed triclosan-loaded MSPMs exhibited a drug leakage when they were suspended in phosphate-buffered saline (PBS) solution [8], albeit at a considerably low rate. To prevent premature drug leakage, strategies such as drug conjugation [120,121], cross-linkage [122–124], and core-shell structure [125–127] have been developed. In these cases, additional stimuli (either external or internal) are needed to trigger the release of cargoes, achieving the so-called 'on-demand' site-specific drug release, which are the subjects of the following sections.

5.3. External stimuli-triggered release nanoparticles

As aforementioned, external stimuli including light, heat, electric, and magnetic fields can be used to control the release of antimicrobials from their carriers spatiotemporally (Fig. 5b).

Light has been extensively explored to enhance the bioavailability and drug efficacy [128], due to its non-invasive and easily manipulated nature. For example, visible light with a wavelength of 600 nm was used to trigger the release of NO from the manganese nitrosyl loaded in porous nanocarriers [129]. Of note, the release of NO from these materials was steady under constant illumination while periodic exposure resulted in the release of pulses of NO. Furthermore, the systems exhibited successful eradication of both drug-susceptible and drug-resistant *Acinetobacter baumannii* in a soft-tissue infection model [129]. The major drawback of UV/visible irradiation is the low tissue penetration depth, less than 1 cm, restricting their applications to superficial tissues instead of the bulk tissues. Near-infrared (NIR) light with a wavelength ranging from 650 to 900 nm can penetrate tissue to a depth of several inches (>500 μm to cm), rendering the NIR light promising for triggering the antimicrobial release in deep tissues [128,130,131].

Photothermal agents such as gold nanoparticles, graphene nanomaterials, and polypyrrole (PPy) nanoparticles are able to generate local heat when they are irradiated by NIR light [132]. This local heat (>45 °C) is lethal to the surrounding pathogens [133] and also used to trigger the release of the loaded antibiotics, synergistically eradicating pathogens. For example, the core-shell-structured hollow microspheres possessing a shell of PLGA and a core of vancomycin and PPy nanoparticles were prepared. The PPy nanoparticles heated the solution to approximately 60.0 °C within 5 min upon NIR irradiation, changing the state of PLGA from glassy state to rubbery state and concurrently triggering the release of vancomycin. Ultimately, the resulting hollow microspheres exhibited synergistic bactericidal efficacy in abscesses *via* the combination of photothermal therapy and antibiotic therapy, outperforming the sum of the two treatments alone [127]. A similar strategy has been applied to construct the gold nanoparticle/silver composites [134]. For example, gold core/silver shell (Au@Ag) nanorods have been developed to combine photothermal therapy and silver toxicity for eradicating *S. epidermidis* or *E. coli* [135]. Recently, a liposome system composed of NIR photothermal agent (cypate), antibiotics (tobramycin) and lipids was fabricated to eliminate *P. aeruginosa* biofilms [136]. In this case, the local heat produced by cypate upon NIR light irradiation induced the dissociation of liposomes resulting in the burst release of antibiotics.

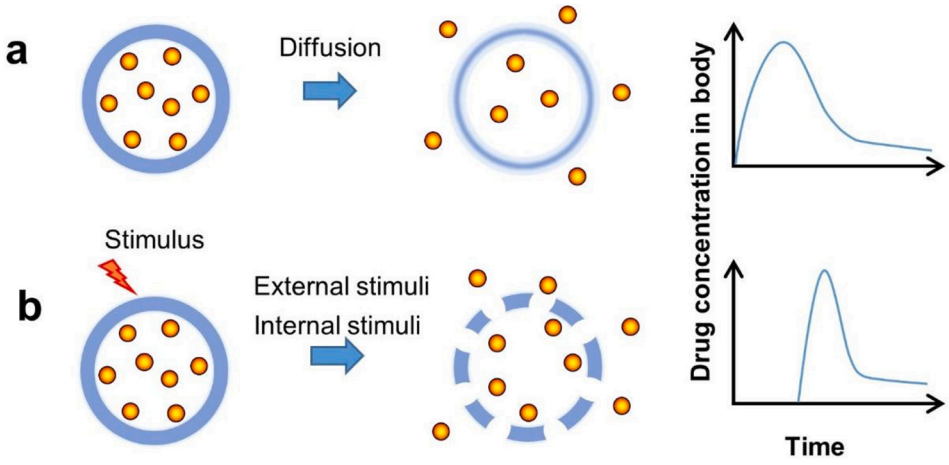

Fig. 5. Main strategies for designing antimicrobial-releasing nanoparticles to control the release of antibacterial agents over space and time. (a) Diffusion-controlled DDS and their antimicrobial release behavior from nanoparticles. (b) Stimulus-controlled DDS and their antimicrobial release behavior from nanoparticles, external stimuli include light, heat, electric, magnetic fields, et al.; internal stimuli include pH and enzymes.

5.4. Internal stimuli-triggered release nanoparticles

Several physiological factors at infection sites could be used as internal stimuli for the release of antimicrobials, as summarized in Table 2.

pH-Responsive nanoparticles. The local acidic microenvironment of a bacterial biofilm has been applied to trigger the release of antimicrobials. In these cases, acidic pH could trigger the protonation of certain segments, inducing the hydrophobic-to-hydrophilic transition which caused the release of the loaded cargoes. For example, block polymer poly(dimethylaminoethyl methacrylate)-*b*-poly(dimethylaminoethyl methacrylate-*co*-butyl methacrylate-*co*-propylacrylic acid) (p(DMAEMA)-*b*-p(DMAEMA-*co*-BMA-*co*-PAA)) was used to construct the pH-responsive polymer nanoparticle carriers (NPCs) which was further used to load farnesol [137,138]. Farnesol was released *via* a pH-dependent manner with $t_{1/2} = 3$ and 15 h for release at pH 4.5 and 7.2, respectively. The loaded farnesol in NPCs was 4-fold more effective in disrupting *Streptococcus mutans* biofilms than free farnesol [137]. We recently developed a pH-responsive antifungal-inbuilt metal-organic-framework to eradicate *C. albicans* biofilms [139]. Antifungals were built-in through the coordination-binding between zinc and antifungals bearing electron-donor segments. The resulting voriconazole-inbuilt zinc 2-methylimidazolates frameworks (V-ZIF) exhibited the pH-dependent zero-order drug release *in vitro*. In an open wound murine model infected by *C. albicans*, V-ZIFs efficiently eradicated the inhabiting fungi and accelerated the wound healing [139]. Besides, pH is also an important factor to influence the assembly and disassembly of nanoparticles in infection control [140,141]. For example, pH-responsive polymer poly(ethylene glycol)-poly(aminopropyl imidazole-aspartate)-polyalanine (PEG-PSB-PALA) was used to condense silver nanoparticles, yielding the silver nanoclusters (AgNCs) that can disassemble in the acidic microenvironment of a biofilm [140].

Enzyme-triggered release systems. Similarly, bacterial lipases [142–145], penicillin G amidase (PGA) and *β*-lactamase (Bla) [146], phospholipase/phosphatase [147] and hyaluronidase [148] -sensitive DDS have been developed. Lipases can hydrolyze polyesters, such as PCL [8,145,149,150] and polyurethanes [151] that provide a hydrophobic environment to stabilize the hydrophobic antimicrobials or confine the hydrophilic antimicrobials to the aqueous interior of a nanocarrier. Therefore, these nanocarriers can be rationally designed into a core-shell polymeric micelle [150,151], a three-layered nanogel [145], or polymersomes [149]. Phosphatases/phospholipases degrade polyphosphoesters that possess a hydrophilic polymer backbone and are suitable for loading hydrophilic antimicrobials [147]. Some notorious bacterial enzymes such as β-lactamases were also used to trigger the release of antibiotics specifically to eradicate the multi-drug resistant pathogenic bacteria and selectively preserve the probiotics [146]. Besides, natural hyaluronic acid could be degraded by hyaluronidase, enabling the construction of the hyaluronidase-responsive antimicrobial-release system. For example, nanoscale metal-organic framework (nMOF) decorated with Ag^{+} and porphyrins exhibited a positive surface charge, which was neutralized by the hyaluronic acid decoration. The hyaluronic acid coating could not only stabilize the encapsulated cargoes but also enable the surface-adaptiveness of the nMOFs. Subsequently, bacterial hyaluronidase triggered the degradation of HA coating, allowing the cationic nMOFs to interact with bacteria [148].

Some toxins can damage the mammalian cell membranes *via* the pore-forming mechanism. Therefore, liposomes loaded with antibiotics are vulnerable in the presence of bacterial toxins and are easy to release the loaded antibiotics [152].

Multiple-responsive systems. As mentioned above, bacterial biofilms are a complex community of bacterial strains. Therefore, it is more efficient to eradicate bacterial biofilms as well as overcome the complex biological barriers *via* multiple-responsive systems. In most cases, multiple responsiveness is designed to overcome the biological barriers in a programmed manner [153]. For example, we loaded antimicrobial triclosan into MSPMs bearing shells composed of PEG and PAE and cores of PCL. Under physiological pH (7.4), the PAE is deprotonated and the whole micelle is stabilized by the stealth PEG shell, facilitating the long circulation and biofilm penetration of micelles. Whereas, PAE is protonated and positively charged in the acidic microenvironment of a biofilm, driving the binds of micelles with bacteria *via* electrostatic interaction. Subsequently, lipase could trigger the dissociation of PCL cores and release of the loaded triclosan to kill the surrounding bacteria

Table 2
Summary of the physiological factors at infection sites that could be used as stimuli for the adaptiveness of biomaterials.

Stimuli	Chemical reactions	Ref.
pH	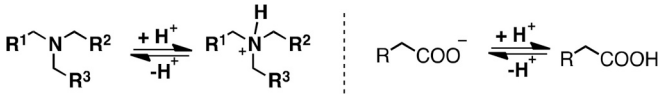	[35,41,154]
Alkaline phosphatase (ALP)	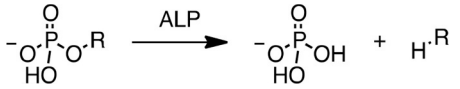	[155]
Lipase	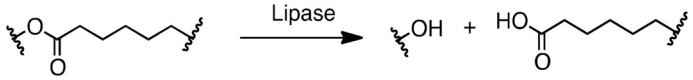	[8,36]
Hyaluronidase	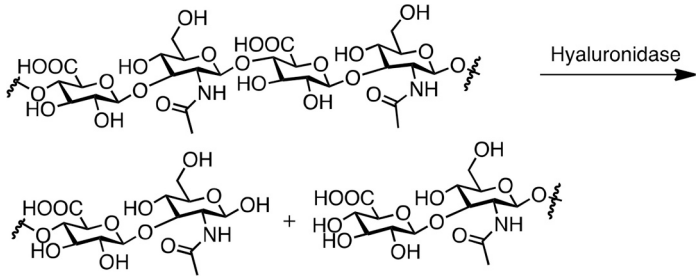	[156]
β-Lactamase	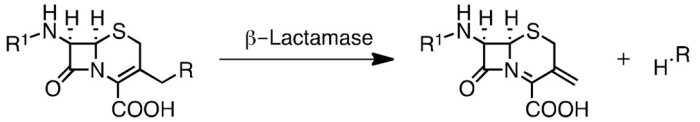	[146]

[8]. To prevent premature drug leakage, we fabricated the triclosan-conjugated PEG-PAE micelles, which also exhibited the pH/lipase dual responsive property and excellent eradication efficacy against both multiple drug-resistant *S. aureus*, *E. coli* and oral streptococcal biofilms [35]. Similarly, Li and coworkers fabricated the vancomycin-conjugated PEG-PCL *via* pH-cleavable hydrazone bonds, which showed pH/lipase-triggered antibiotic release profiles [150].

6. Conclusions and perspectives

In the past decades, numerous advanced drug delivery and release systems have been developed to relieve bacterial infections, especially for those associated with biofilms. In this review, we summarized the mathematical models and principles of building the controlled DDS, as well as the recently developed controlled DDS for the diversity of antimicrobials. Nevertheless, the following critical issues remain to be addressed to better translate the controlled DDS from bench to bedside.

(1) Although the zero-order release systems seem to be outdated, the advantages of zero-order release are obvious, such as maintaining the drug concentration in the blood or tissues at the desired value for a certain duration. Besides, drug release kinetics could be quantitatively predicted before applied. Zero-order release DDS can be rejuvenated by the incorporation of stimuli-responsive segments, as the developed two platforms which release cargoes *via* a stimuli-responsive zero-order release profile [139,157]. However, there is no doubt that more novel and adapted techniques are still needed.
(2) The use of antimicrobials will inevitably cause bacterial resistance. Thus, non-antimicrobial-based treatments, such as biomimetic enzymes [158,159] and GO-based active agents/delivery systems [160,161], have great potential in overcoming and preventing the emergence of drug resistance.
(3) The administered nanomedicines often suffered from low bioavailability, due partially to their considerably short half-lives in blood circulation, which may strongly impede their clinical translation.
(4) Although electrospun fibers have demonstrated their potential in drug delivery and controlled release, their application in antimicrobial delivery especially in combating bacteria in their biofilm-mode of growth is still in infancy.
(5) Another challenging issue is to fabricate a large variety of antimicrobial composites in a convenient, reproducible, large scale, cost-effective way.
(6) It is also necessary to develop novel strategies that enable the eradication of bacteria while minimizing the damage to the normal tissues.

We believe that through our continuous efforts, we can minimize the emergence of drug-resistant bacteria, extend the use period of our existing antibiotic library, develop better antimicrobials and their delivery systems, to benefit patients.

Acknowledgments

This work was financially supported by the National Natural Science Foundation of China (Nos. 21620102005, 51933006, 52003184), and the State Key Laboratory of Medicinal Chemical Biology (Grant No. 2019016), Nankai University.

References

[1] J. O'Neill, Antimicrobial resistance: tackling a crisis for the health and wealth of nations, Rev. Antimicrob. Resist. 20 (2014) 1–16.
[2] P. Fernandes, Antibacterial discovery and development—the failure of success? Nat. Biotechnol. 24 (2006) 1497–1503, https://doi.org/10.1038/nbt1206-1497.
[3] A.J. Alanis, Resistance to antibiotics: are we in the post-antibiotic era? Arch. Med. Res. 36 (2005) 697–705, https://doi.org/10.1016/j.arcmed.2005.06.009.
[4] D. Davies, Understanding biofilm resistance to antibacterial agents, Nat. Rev. Drug Discov. 2 (2003) 114–122, https://doi.org/10.1038/nrd1008.
[5] Y. Liu, L. Shi, L. Su, H.C. van der Mei, P.C. Jutte, Y. Ren, H.J. Busscher, Nanotechnology-based antimicrobials and delivery systems for biofilm-infection control, Chem. Soc. Rev. 48 (2019) 428–446, https://doi.org/10.1039/C7CS00807D.
[6] C.W. Hall, T.F. Mah, Molecular mechanisms of biofilm-based antibiotic resistance and tolerance in pathogenic bacteria, FEMS Microbiol. Rev. 41 (2017) 276–301, https://doi.org/10.1093/femsre/fux010.
[7] H.-C. Flemming, J. Wingender, U. Szewzyk, P. Steinberg, S.A. Rice, S. Kjelleberg, Biofilms: An emergent form of bacterial life, Nat. Rev. Microbiol. 14 (2016) 563–575, https://doi.org/10.1038/nrmicro.2016.94.
[8] Y. Liu, H.J. Busscher, B. Zhao, Y. Li, Z. Zhang, H.C. Van Der Mei, Y. Ren, L. Shi, Surface-adaptive, antimicrobially loaded, micellar nanocarriers with enhanced penetration and killing efficiency in Staphylococcal biofilms, ACS Nano 10 (2016) 4779–4789, https://doi.org/10.1021/acsnano.6b01370.
[9] K. Park, Controlled drug delivery systems: past forward and future back, J. Control. Release 190 (2014) 3–8, https://doi.org/10.1016/j.jconrel.2014.03.054.
[10] V. Vijayakumar, K.G. Subramanian, Drug carriers, polymers as: synthesis, characterization, and in vitro evaluation, in: Encycl. Biomed. Polym. Polym. Biomater, Taylor & Francis, 2016, pp. 1–28, https://doi.org/10.1081/E-EBPP-120050597.
[11] B. Narasimhan, R. Langer, Zero-order release of micro- and macromolecules from polymeric devices: the role of the burst effect, J. Control. Release 47 (1997) 13–20, https://doi.org/10.1016/S0168-3659(96)01611-2.
[12] N.A. Peppas, B. Narasimhan, Mathematical models in drug delivery: how modeling has shaped the way we design new drug delivery systems, J. Control. Release 190 (2014) 75–81, https://doi.org/10.1016/j.jconrel.2014.06.041.
[13] J. Siepmann, F. Siepmann, Mathematical modeling of drug dissolution, Int. J. Pharm. 453 (2013) 12–24, https://doi.org/10.1016/j.ijpharm.2013.04.044.
[14] A. Fick, Ueber diffusion, Ann. Der Phys. Und Chem. 170 (1855) 59–86, https://doi.org/10.1002/andp.18551700105.
[15] J.W. Westwater, H.G. Drickamer, The mathematics of diffusion, J. Am. Chem. Soc. 79 (1957) 1267–1268, https://doi.org/10.1021/ja01562a072.
[16] J. Siepmann, F. Siepmann, Modeling of diffusion controlled drug delivery, J. Control. Release 161 (2012) 351–362, https://doi.org/10.1016/j.jconrel.2011.10.006.
[17] B. Narasimhan, Mathematical models describing polymer dissolution: consequences for drug delivery, Adv. Drug Deliv. Rev. 48 (2001) 195–210, https://doi.org/10.1016/S0169-409X(01)00117-X.
[18] B. Narasimhan, N.A. Peppas, Molecular analysis of drug delivery systems controlled by dissolution of the polymer carrier, J. Pharm. Sci. 86 (1997) 297–304, https://doi.org/10.1021/js960372z.
[19] J. Siepmann, A. Gopferich, Mathematical modeling of bioerodible, polymeric drug delivery systems, Adv. Drug Deliv. Rev. 48 (2001) 229–247, https://doi.org/10.1016/S0169-409X(01)00116-8.
[20] N. Kamaly, B. Yameen, J. Wu, O.C. Farokhzad, Degradable controlled-release polymers and polymeric nanoparticles: mechanisms of controlling drug release, Chem. Rev. 116 (2016) 2602–2663, https://doi.org/10.1021/acs.chemrev.5b00346.
[21] H.B. Hopfenberg, Controlled release from erodible slabs, cylinders, and spheres, in: Control. Release Polym. Formul, 1976, pp. 26–32, https://doi.org/10.1021/bk-1976-0033.ch003.
[22] D.O. Cooney, Effect of geometry on the dissolution of pharmaceutical tablets and other solids: surface detachment kinetics controlling, AICHE J. 18 (1972) 446–449, https://doi.org/10.1002/aic.690180234.
[23] H. Karasulu, Modeling of theophylline release from different geometrical erodible tablets, Eur. J. Pharm. Biopharm. 49 (2000) 177–182, https://doi.org/10.1016/S0939-6411(99)00082-X.
[24] C. Aguzzi, P. Cerezo, I. Salcedo, R. Sánchez, C. Viseras, Mathematical models describing drug release from biopolymeric delivery systems, Mater. Technol. 25 (2010) 205–211, https://doi.org/10.1179/175355510X12723642365566.
[25] L.L. Lao, S.S. Venkatraman, N.A. Peppas, Modeling of drug release from biodegradable polymer blends, Eur. J. Pharm. Biopharm. 70 (2008) 796–803, https://doi.org/10.1016/j.ejpb.2008.05.024.
[26] J. Siepmann, H. Kranz, R. Bodmeier, N.A. Peppas, HPMC-matrices for controlled drug delivery: a new model combining diffusion, swelling, and dissolution mechanisms and predicting the release kinetics, Pharm. Res. 16 (1999) 1748–1756, https://doi.org/10.1023/A:1018914301328.
[27] E.M. Hetrick, M.H. Schoenfisch, Reducing implant-related infections: active release strategies, Chem. Soc. Rev. 35 (2006) 780–789, https://doi.org/10.1039/b515219b.
[28] C.R. Arciola, D. Campoccia, L. Montanaro, Implant infections: adhesion, biofilm formation and immune evasion, Nat. Rev. Microbiol. 16 (2018) 397–409, https://doi.org/10.1038/s41579-018-0019-y.
[29] R. Kaur, S. Liu, Antibacterial surface design – contact kill, Prog. Surf. Sci. 91 (2016) 136–153, https://doi.org/10.1016/j.progsurf.2016.09.001.
[30] J.C. Tiller, C.-J. Liao, K. Lewis, A.M. Klibanov, Designing surfaces that kill bacteria on contact, Proc. Natl. Acad. Sci. 98 (2001) 5981–5985, https://doi.org/10.1073/pnas.111143098.
[31] T. Wei, Q. Yu, H. Chen, Responsive and synergistic antibacterial coatings: fighting against bacteria in a smart and effective way, Adv. Healthc. Mater. 8 (2019) 1801381, https://doi.org/10.1002/adhm.201801381.

[32] V.B. Damodaran, N.S. Murthy, Bio-inspired strategies for designing antifouling biomaterials, Biomater. Res. 20 (2016) 18, https://doi.org/10.1186/s40824-016-0064-4.
[33] L.D. Blackman, P.A. Gunatillake, P. Cass, K.E.S. Locock, An introduction to zwitterionic polymer behavior and applications in solution and at surfaces, Chem. Soc. Rev. 48 (2019) 757–770, https://doi.org/10.1039/C8CS00508G.
[34] N.J. Hickok, I.M. Shapiro, Immobilized antibiotics to prevent orthopaedic implant infections, Adv. Drug Deliv. Rev. 64 (2012) 1165–1176, https://doi.org/10.1016/j.addr.2012.03.015.
[35] Y. Liu, Y. Ren, Y. Li, L. Su, Y. Zhang, F. Huang, J. Liu, J. Liu, T.G. van Kooten, Y. An, L. Shi, H.C. van der Mei, H.J. Busscher, Nanocarriers with conjugated antimicrobials to eradicate pathogenic biofilms evaluated in murine in vivo and human ex vivo infection models, Acta Biomater. 79 (2018) 331–343, https://doi.org/10.1016/j.actbio.2018.08.038.
[36] V.V. Komnatnyy, W.C. Chiang, T. Tolker-Nielsen, M. Givskov, T.E. Nielsen, Bacteria-triggered release of antimicrobial agents, Angew. Chem. Int. Ed. 53 (2014) 439–441, https://doi.org/10.1002/anie.201307975.
[37] J. Hirschfeld, E.M. Akinoglu, D.C. Wirtz, A. Hoerauf, I. Bekeredjian-Ding, S. Jepsen, E.M. Haddouti, A. Limmer, M. Giersig, Long-term release of antibiotics by carbon nanotube-coated titanium alloy surfaces diminish biofilm formation by *Staphylococcus epidermidis*, Nanomed. Nanotechnol. Biol. Med. 13 (2017) 1587–1593, https://doi.org/10.1016/j.nano.2017.01.002.
[38] H.F. Chuang, R.C. Smith, P.T. Hammond, Polyelectrolyte multilayers for tunable release of antibiotics, Biomacromolecules 9 (2008) 1660–1668, https://doi.org/10.1021/bm800185h.
[39] J.S. Moskowitz, M.R. Blaisse, R.E. Samuel, H.-P. Hsu, M.B. Harris, S.D. Martin, J. C. Lee, M. Spector, P.T. Hammond, The effectiveness of the controlled release of gentamicin from polyelectrolyte multilayers in the treatment of *Staphylococcus aureus* infection in a rabbit bone model, Biomaterials 31 (2010) 6019–6030, https://doi.org/10.1016/j.biomaterials.2010.04.011.
[40] V. Bansal, P.K. Sharma, N. Sharma, O.P. Pal, R. Malviya, Applications of chitosan and chitosan derivatives in drug delivery, Biol. Res. 5 (2011) 28–37, https://doi.org/10.1007/12.
[41] Y. Liu, Y.F. Li, D. Keskin, L. Shi, Poly(β-amino esters): synthesis, formulations, and their biomedical applications, Adv. Healthc. Mater. 8 (2019) 1801359, https://doi.org/10.1002/adhm.201801359.
[42] A. Shukla, S.N. Avadhany, J.C. Fang, P.T. Hammond, Tunable vancomycin releasing surfaces for biomedical applications, Small 6 (2010) 2392–2404, https://doi.org/10.1002/smll.201001150.
[43] G. Cado, R. Aslam, L. Séon, T. Garnier, R. Fabre, A. Parat, A. Chassepot, J. C. Voegel, B. Senger, F. Schneider, Y. Frère, L. Jierry, P. Schaaf, H. Kerdjoudj, M. H. Metz-Boutigue, F. Boulmedais, Self-defensive biomaterial coating against bacteria and yeasts: polysaccharide multilayer film with embedded antimicrobial peptide, Adv. Funct. Mater. 23 (2013) 4801–4809, https://doi.org/10.1002/adfm.201300416.
[44] A. Shukla, K.E. Fleming, H.F. Chuang, T.M. Chau, C.R. Loose, G. N. Stephanopoulos, P.T. Hammond, Controlling the release of peptide antimicrobial agents from surfaces, Biomaterials 31 (2010) 2348–2357, https://doi.org/10.1016/j.biomaterials.2009.11.082.
[45] A.W. Carpenter, M.H. Schoenfisch, Nitric oxide release: part II. Therapeutic applications, Chem. Soc. Rev. 41 (2012) 3742–3752, https://doi.org/10.1039/c2cs15273h.
[46] N. Barraud, M. Kelso, S. Rice, S. Kjelleberg, Nitric oxide: a key mediator of biofilm dispersal with applications in infectious diseases, Curr. Pharm. Des. 21 (2014) 31–42, https://doi.org/10.2174/13816128206661409051128 22.
[47] T. Yang, A.N. Zelikin, R. Chandrawati, Progress and promise of nitric oxide-releasing platforms, Adv. Sci. 5 (2018) 1701043, https://doi.org/10.1002/advs.201701043.
[48] J.A. Hrabie, L.K. Keefer, Chemistry of the nitric oxide-releasing diazeniumdiolate ("nitrosohydroxylamine") functional group and its oxygen-substituted derivatives, Chem. Rev. 102 (2002) 1135–1154, https://doi.org/10.1021/cr000028t.
[49] W. Cai, J. Wu, C. Xi, M.E. Meyerhoff, Diazeniumdiolate-doped poly(lactic-co-glycolic acid)-based nitric oxide releasing films as antibiofilm coatings, Biomaterials 33 (2012) 7933–7944, https://doi.org/10.1016/j.biomaterials.2012.07.027.
[50] L.C. Xu, Y. Wo, M.E. Meyerhoff, C.A. Siedlecki, Inhibition of bacterial adhesion and biofilm formation by dual functional textured and nitric oxide releasing surfaces, Acta Biomater. 51 (2017) 53–65, https://doi.org/10.1016/j.actbio.2017.01.030.
[51] S.P. Hopkins, J. Pant, M.J. Goudie, C. Schmiedt, H. Handa, Achieving long-term biocompatible silicone via covalently immobilized S-Nitroso- N-acetylpenicillamine (SNAP) that exhibits 4 months of sustained nitric oxide release, ACS Appl. Mater. Interfaces 10 (2018) 27316–27325, https://doi.org/10.1021/acsami.8b08647.
[52] Z. Sadrearhami, F.N. Shafiee, K.K.K. Ho, N. Kumar, M. Krasowska, A. Blencowe, E.H.H. Wong, C. Boyer, Antibiofilm nitric oxide-releasing polydopamine coatings, ACS Appl. Mater. Interfaces 11 (2019) 7320–7329, https://doi.org/10.1021/acsami.8b16853.
[53] M. Cloutier, D. Mantovani, F. Rosei, Antibacterial coatings: challenges, perspectives, and opportunities, Trends Biotechnol. 33 (2015) 637–652, https://doi.org/10.1016/j.tibtech.2015.09.002.
[54] S.M. Dizaj, F. Lotfipour, M. Barzegar-Jalali, M.H. Zarrintan, K. Adibkia, Antimicrobial activity of the metals and metal oxide nanoparticles, Mater. Sci. Eng. C 44 (2014) 278–284, https://doi.org/10.1016/j.msec.2014.08.031.
[55] R. Kumar, H. Münstedt, Silver ion release from antimicrobial polyamide/silver composites, Biomaterials 26 (2005) 2081–2088, https://doi.org/10.1016/j.biomaterials.2004.05.030.
[56] J.A. Lemire, J.J. Harrison, R.J. Turner, Antimicrobial activity of metals: mechanisms, molecular targets and applications, Nat. Rev. Microbiol. 11 (2013) 371–384, https://doi.org/10.1038/nrmicro3028.
[57] J. Raphel, M. Holodniy, S.B. Goodman, S.C. Heilshorn, Multifunctional coatings to simultaneously promote osseointegration and prevent infection of orthopaedic implants, Biomaterials 84 (2016) 301–314, https://doi.org/10.1016/j.biomaterials.2016.01.016.
[58] A. Kumar, P.K. Vemula, P.M. Ajayan, G. John, Silver-nanoparticle-embedded antimicrobial paints based on vegetable oil, Nat. Mater. 7 (2008) 236–241, https://doi.org/10.1038/nmat2099.
[59] B. Le Ouay, F. Stellacci, Antibacterial activity of silver nanoparticles: a surface science insight, Nano Today 10 (2015) 339–354, https://doi.org/10.1016/j.nantod.2015.04.002.
[60] H. Qin, H. Cao, Y. Zhao, C. Zhu, T. Cheng, Q. Wang, X. Peng, M. Cheng, J. Wang, G. Jin, Y. Jiang, X. Zhang, X. Liu, P.K. Chu, In vitro and in vivo anti-biofilm effects of silver nanoparticles immobilized on titanium, Biomaterials 35 (2014) 9114–9125, https://doi.org/10.1016/j.biomaterials.2014.07.040.
[61] W.A. Daoud, J.H. Xin, Y.-H. Zhang, Surface functionalization of cellulose fibers with titanium dioxide nanoparticles and their combined bactericidal activities, Surf. Sci. 599 (2005) 69–75, https://doi.org/10.1016/j.susc.2005.09.038.
[62] A. Sirelkhatim, S. Mahmud, A. Seeni, N.H.M. Kaus, L.C. Ann, S.K.M. Bakhori, H. Hasan, D. Mohamad, Review on zinc oxide nanoparticles: antibacterial activity and toxicity mechanism, Nano-Micro Lett. 7 (2015) 219–242, https://doi.org/10.1007/s40820-015-0040-x.
[63] H.M.A. Ehmann, D. Breitwieser, S. Winter, C. Gspan, G. Koraimann, U. Maver, M. Sega, S. Köstler, K. Stana-Kleinschek, S. Spirk, Gold nanoparticles in the engineering of antibacterial and anticoagulant surfaces, Carbohydr. Polym. 117 (2015) 34–42, https://doi.org/10.1016/j.carbpol.2014.08.116.
[64] A. Rai, A. Prabhune, C.C. Perry, Antibiotic mediated synthesis of gold nanoparticles with potent antimicrobial activity and their application in antimicrobial coatings, J. Mater. Chem. 20 (2010) 6789, https://doi.org/10.1039/c0jm00817f.
[65] H. Cheng, Y. Xie, L.F. Villalobos, L. Song, K.-V. Peinemann, S. Nunes, P.-Y. Hong, Antibiofilm effect enhanced by modification of 1,2,3-triazole and palladium nanoparticles on polysulfone membranes, Sci. Rep. 6 (2016) 24289, https://doi.org/10.1038/srep24289.
[66] C.P. Adams, K.A. Walker, S.O. Obare, K.M. Docherty, Size-dependent antimicrobial effects of novel palladium nanoparticles, PLoS One 9 (2014), e85981, https://doi.org/10.1371/journal.pone.0085981.
[67] Y. Wang, D.S. Kohane, External triggering and triggered targeting strategies for drug delivery, Nat. Rev. Mater. 2 (2017), https://doi.org/10.1038/natrevmats.2017.20.
[68] G. Gao, Y.W. Jiang, H.R. Jia, F.G. Wu, Near-infrared light-controllable on-demand antibiotics release using thermo-sensitive hydrogel-based drug reservoir for combating bacterial infection, Biomaterials 188 (2019) 83–95, https://doi.org/10.1016/j.biomaterials.2018.09.045.
[69] L.J. Delaney, D. MacDonald, J. Leung, K. Fitzgerald, A.M. Sevit, J.R. Eisenbrey, N. Patel, F. Forsberg, C.K. Kepler, T. Fang, S.M. Kurtz, N.J. Hickok, Ultrasound-triggered antibiotic release from PEEK clips to prevent spinal fusion infection: initial evaluations, Acta Biomater. 93 (2019) 12–24, https://doi.org/10.1016/j.actbio.2019.02.041.
[70] P. Norris, M. Noble, I. Francolini, A.M. Vinogradov, P.S. Stewart, B.D. Ratner, J. W. Costerton, P. Stoodley, Ultrasonically controlled release of ciprofloxacin from self-assembled coatings on poly(2-hydroxyethyl methacrylate) hydrogels for *Pseudomonas aeruginosa* biofilm prevention, Antimicrob. Agents Chemother. 49 (2005) 4272–4279, https://doi.org/10.1128/AAC.49.10.4272-4279.2005.
[71] D.J. Schmidt, J.S. Moskowitz, P.T. Hammond, Electrically triggered release of a small molecule drug from a polyelectrolyte multilayer coating, Chem. Mater. 22 (2010) 6416–6425, https://doi.org/10.1021/cm102578j.
[72] X. Shi, H. Wu, Y. Li, X. Wei, Y. Du, Electrical signals guided entrapment and controlled release of antibiotics on titanium surface, J. Biomed. Mater. Res. A 101 (A) (2013) 1373–1378, https://doi.org/10.1002/jbm.a.34432.
[73] S. Szunerits, F. Teodorescu, R. Boukherroub, Electrochemically triggered release of drugs, Eur. Polym. J. 83 (2016) 467–477, https://doi.org/10.1016/j.eurpolymj.2016.03.001.
[74] X. Wang, A. Deng, W. Cao, Q. Li, L. Wang, J. Zhou, B. Hu, X. Xing, Synthesis of chitosan/poly (ethylene glycol)-modified magnetic nanoparticles for antibiotic delivery and their enhanced anti-biofilm activity in the presence of magnetic field, J. Mater. Sci. 53 (2018) 6433–6449, https://doi.org/10.1007/s10853-018-1998-9.
[75] L. Su, Y. Li, Y. Liu, Y. An, L. Shi, Recent advances and future prospects on adaptive biomaterials for antimicrobial applications, Macromol. Biosci. 19 (2019) 1900289, https://doi.org/10.1002/mabi.201900289.
[76] I. Zhuk, F. Jariwala, A.B. Attygalle, Y. Wu, M.R. Libera, S.A. Sukhishvili, Self-defensive layer-by-layer films with bacteria-triggered antibiotic release, ACS Nano 8 (2014) 7733–7745, https://doi.org/10.1021/nn500674g.
[77] T. Wang, C. Wang, S. Zhou, J. Xu, W. Jiang, L. Tan, J. Fu, Nanovalves-based bacteria-triggered, self-defensive antibacterial coating: using combination therapy, dual stimuli-responsiveness, and multiple release modes for treatment of implant-associated infections, Chem. Mater. 29 (2017) 8325–8337, https://doi.org/10.1021/acs.chemmater.7b02678.

[78] S.F. Chou, D. Carson, K.A. Woodrow, Current strategies for sustaining drug release from electrospun nanofibers, J. Control. Release 220 (2015) 584–591, https://doi.org/10.1016/j.jconrel.2015.09.008.
[79] M. Zamani, M.P. Prabhakaran, S. Ramakrishna, Advances in drug delivery via electrospun and electrosprayed nanomaterials, Int. J. Nanomedicine 8 (2013) 2997–3017, https://doi.org/10.2147/IJN.S43575.
[80] S. Chen, R. Li, X. Li, J. Xie, Electrospinning: An enabling nanotechnology platform for drug delivery and regenerative medicine, Adv. Drug Deliv. Rev. 132 (2018) 188–213, https://doi.org/10.1016/j.addr.2018.05.001.
[81] G. Yang, X. Li, Y. He, J. Ma, G. Ni, S. Zhou, From nano to micro to macro: electrospun hierarchically structured polymeric fibers for biomedical applications, Prog. Polym. Sci. 81 (2018) 80–113, https://doi.org/10.1016/j.progpolymsci.2017.12.003.
[82] X. Hu, S. Liu, G. Zhou, Y. Huang, Z. Xie, X. Jing, Electrospinning of polymeric nanofibers for drug delivery applications, J. Control. Release 185 (2014) 12–21, https://doi.org/10.1016/j.jconrel.2014.04.018.
[83] T.J. Sill, H.A. von Recum, Electrospinning: applications in drug delivery and tissue engineering, Biomaterials 29 (2008) 1989–2006, https://doi.org/10.1016/j.biomaterials.2008.01.011.
[84] Y. Yang, W. Li, D.G. Yu, G. Wang, G.R. Williams, Z. Zhang, Tunable drug release from nanofibers coated with blank cellulose acetate layers fabricated using tri-axial electrospinning, Carbohydr. Polym. 203 (2019) 228–237, https://doi.org/10.1016/j.carbpol.2018.09.061.
[85] D. Han, S. Sherman, S. Filocamo, A.J. Steckl, Long-term antimicrobial effect of nisin released from electrospun triaxial fiber membranes, Acta Biomater. 53 (2017) 242–249, https://doi.org/10.1016/j.actbio.2017.02.029.
[86] X. Liu, Y. Yang, D.G. Yu, M.J. Zhu, M. Zhao, G.R. Williams, Tunable zero-order drug delivery systems created by modified triaxial electrospinning, Chem. Eng. J. 356 (2019) 886–894, https://doi.org/10.1016/j.cej.2018.09.096.
[87] K. Kim, Y.K. Luu, C. Chang, D. Fang, B.S. Hsiao, B. Chu, M. Hadjiargyrou, Incorporation and controlled release of a hydrophilic antibiotic using poly (lactide-co-glycolide)-based electrospun nanofibrous scaffolds, J. Control. Release 98 (2004) 47–56, https://doi.org/10.1016/j.jconrel.2004.04.009.
[88] A.C. Alavarse, F.W. de Oliveira Silva, J.T. Colque, V.M. da Silva, T. Prieto, E. C. Venancio, J.J. Bonvent, Tetracycline hydrochloride-loaded electrospun nanofibers mats based on PVA and chitosan for wound dressing, Mater. Sci. Eng. C 77 (2017) 271–281, https://doi.org/10.1016/j.msec.2017.03.199.
[89] A.F. De Faria, F. Perreault, E. Shaulsky, L.H. Arias Chavez, M. Elimelech, Antimicrobial electrospun biopolymer nanofiber mats functionalized with graphene oxide-silver nanocomposites, ACS Appl. Mater. Interfaces 7 (2015) 12751–12759, https://doi.org/10.1021/acsami.5b01639.
[90] S. Torres-Giner, M.J. Ocio, J.M. Lagaron, Novel antimicrobial ultrathin structures of zein/chitosan blends obtained by electrospinning, Carbohydr. Polym. 77 (2009) 261–266, https://doi.org/10.1016/j.carbpol.2008.12.035.
[91] J. Miao, R.C. Pangule, E.E. Paskaleva, E.E. Hwang, R.S. Kane, R.J. Linhardt, J. S. Dordick, Lysostaphin-functionalized cellulose fibers with antistaphylococcal activity for wound healing applications, Biomaterials 32 (2011) 9557–9567, https://doi.org/10.1016/j.biomaterials.2011.08.080.
[92] M. Reise, R. Wyrwa, U. Müller, M. Zylinski, A. Völpel, M. Schnabelrauch, A. Berg, K.D. Jandt, D.C. Watts, B.W. Sigusch, Release of metronidazole from electrospun poly(l-lactide-co-d/l-lactide) fibers for local periodontitis treatment, Dent. Mater. 28 (2012) 179–188, https://doi.org/10.1016/j.dental.2011.12.006.
[93] R. Qi, R. Guo, F. Zheng, H. Liu, J. Yu, X. Shi, Controlled release and antibacterial activity of antibiotic-loaded electrospun halloysite/poly(lactic-co-glycolic acid) composite nanofibers, Colloids Surf. B Biointerf. 110 (2013) 148–155, https://doi.org/10.1016/j.colsurfb.2013.04.036.
[94] Z. Zhang, J. Tang, H. Wang, Q. Xia, S. Xu, C.C. Han, Controlled antibiotics release system through simple blended electrospun fibers for sustained antibacterial effects, ACS Appl. Mater. Interfaces 7 (2015) 26400–26404, https://doi.org/10.1021/acsami.5b09820.
[95] S. Nagarajan, L. Soussan, M. Bechelany, C. Teyssier, V. Cavaillès, C. Pochat-Bohatier, P. Miele, N. Kalkura, J.M. Janot, S. Balme, Novel biocompatible electrospun gelatin fiber mats with antibiotic drug delivery properties, J. Mater. Chem. B 4 (2016) 1134–1141, https://doi.org/10.1039/c5tb01897h.
[96] S.M. Ahmed, H. Ahmed, C. Tian, Q. Tu, Y. Guo, J. Wang, Whey protein concentrate doped electrospun poly(epsilon-caprolactone) fibers for antibiotic release improvement, Colloids Surf. B Biointerf. 143 (2016) 371–381, https://doi.org/10.1016/j.colsurfb.2016.03.059.
[97] X. Yang, J. Yang, L. Wang, B. Ran, Y. Jia, L. Zhang, G. Yang, H. Shao, X. Jiang, Pharmaceutical intermediate-modified gold nanoparticles: against multidrug-resistant bacteria and wound-healing application via an electrospun scaffold, ACS Nano 11 (2017) 5737–5745, https://doi.org/10.1021/acsnano.7b01240.
[98] I. Altinbasak, R. Jijie, A. Barras, B. Golba, R. Sanyal, J. Bouckaert, D. Drider, R. Bilyy, T. Dumych, S. Paryzhak, V. Vovk, R. Boukherroub, A. Sanyal, S. Szunerits, Reduced graphene-oxide-embedded polymeric nanofiber mats: an "on-demand" photothermally triggered antibiotic release platform, ACS Appl. Mater. Interfaces 10 (2018) 41098–41106, https://doi.org/10.1021/acsami.8b14784.
[99] T.T.T. Nguyen, O.H. Chung, J.S. Park, Coaxial electrospun poly(lactic acid)/chitosan (core/shell) composite nanofibers and their antibacterial activity, Carbohydr. Polym. 86 (2011) 1799–1806, https://doi.org/10.1016/j.carbpol.2011.07.014.
[100] K. Kalwar, W.X. Sun, D.L. Li, X.J. Zhang, D. Shan, Coaxial electrospinning of polycaprolactone@chitosan: characterization and silver nanoparticles incorporation for antibacterial activity, React. Funct. Polym. 107 (2016) 87–92, https://doi.org/10.1016/j.reactfunctpolym.2016.08.010.
[101] J. Yang, K. Wang, D.G. Yu, Y. Yang, S.W.A. Bligh, G.R. Williams, Electrospun Janus nanofibers loaded with a drug and inorganic nanoparticles as an effective antibacterial wound dressing, Mater. Sci. Eng. C 111 (2020) 110805, https://doi.org/10.1016/j.msec.2020.110805.
[102] H. Rodríguez-Tobías, G. Morales, D. Grande, Comprehensive review on electrospinning techniques as versatile approaches toward antimicrobial biopolymeric composite fibers, Mater. Sci. Eng. C 101 (2019) 306–322, https://doi.org/10.1016/j.msec.2019.03.099.
[103] H.S. Choi, W. Liu, P. Misra, E. Tanaka, J.P. Zimmer, B.I. Ipe, M.G. Bawendi, J. V. Frangioni, Renal clearance of nanoparticles, Nat. Biotechnol. 25 (2007) 1165, https://doi.org/10.1038/nbt1340.
[104] E. Blanco, H. Shen, M. Ferrari, Principles of nanoparticle design for overcoming biological barriers to drug delivery, Nat. Biotechnol. 33 (2015) 941–951, https://doi.org/10.1038/nbt.3330.
[105] Y. Liu, H.C. van der Mei, B. Zhao, Y. Zhai, T. Cheng, Y. Li, Z. Zhang, H.J. Busscher, Y. Ren, L. Shi, Eradication of multidrug-resistant staphylococcal infections by light-activatable micellar nanocarriers in a murine model, Adv. Funct. Mater. 27 (2017) 1701974, https://doi.org/10.1002/adfm.201701974.
[106] R. Kamata, T. Yamamoto, K. Matsumoto, H. Maeda, A serratial protease causes vascular permeability reaction by activation of the Hageman factor-dependent pathway in Guinea pigs, Infect. Immun. 48 (1985) 747–753, https://doi.org/10.1128/IAI.48.3.747-753.1985.
[107] Y. Ding, Y. Xu, W. Yang, P. Niu, X. Li, Y. Chen, Z. Li, Y. Liu, Y. An, Y. Liu, W. Shen, L. Shi, Investigating the EPR effect of nanomedicines in human renal tumors via ex vivo perfusion strategy, Nano Today 35 (2020) 100970, https://doi.org/10.1016/j.nantod.2020.100970.
[108] Y. Li, G. Yang, Y. Ren, L. Shi, R. Ma, H.C. van der Mei, H.J. Busscher, Applications and perspectives of cascade reactions in bacterial infection control, Front. Chem. 7 (2020) 861, https://doi.org/10.3389/fchem.2019.00861.
[109] Y. Li, Y. Liu, Y. Ren, L. Su, A. Li, Y. An, V. Rotello, Z. Zhang, Y. Wang, Y. Liu, S. Liu, J. Liu, J.D. Laman, L. Shi, H.C. van der Mei, H.J. Busscher, Coating of a novel antimicrobial nanoparticle with a macrophage membrane for the selective entry into infected macrophages and killing of intracellular Staphylococci, Adv. Funct. Mater. (2020) 2004942, https://doi.org/10.1002/adfm.202004942, n/a.
[110] M. Natan, E. Banin, From nano to micro: using nanotechnology to combat microorganisms and their multidrug resistance, FEMS Microbiol. Rev. 41 (2017) 302–322, https://doi.org/10.1093/femsre/fux003.
[111] P.V. Baptista, M.P. McCusker, A. Carvalho, D.A. Ferreira, N.M. Mohan, M. Martins, A.R. Fernandes, Nano-strategies to fight multidrug resistant bacteria-"a battle of the titans", Front. Microbiol. 9 (2018) 1–26, https://doi.org/10.3389/fmicb.2018.01441.
[112] H. Koo, R.N. Allan, R.P. Howlin, P. Stoodley, L. Hall-Stoodley, Targeting microbial biofilms: current and prospective therapeutic strategies, Nat. Rev. Microbiol. 15 (2017) 740–755, https://doi.org/10.1038/nrmicro.2017.99.
[113] X. Zhang, L.Y. Wang, J.F. Xu, D.Y. Chen, L.Q. Shi, Y.F. Zhou, Z.H. Shen, Polymeric supramolecular systems: design, assembly and functions, Acta Polym. Sin. 50 (2019) 973–987, https://doi.org/10.11777/j.issn1000-3304.2019.19109.
[114] M.A.S. Melo, S.F.F. Guedes, H.H.K. Xu, L.K.A. Rodrigues, Nanotechnology-based restorative materials for dental caries management, Trends Biotechnol. 31 (2013) 459–467, https://doi.org/10.1016/j.tibtech.2013.05.010.
[115] L. Rizzello, R. Cingolani, P.P. Pompa, Nanotechnology tools for antibacterial materials, Nanomedicine 8 (2013) 807–821, https://doi.org/10.2217/nnm.13.63.
[116] Z. Drulis-Kawa, A. Dorotkiewicz-Jach, Liposomes as delivery systems for antibiotics, Int. J. Pharm. 387 (2010) 187–198, https://doi.org/10.1016/j.ijpharm.2009.11.033.
[117] Z. Gounani, M.A. Asadollahi, J.N. Pedersen, J. Lyngsø, J. Skov Pedersen, A. Arpanaei, R.L. Meyer, Mesoporous silica nanoparticles carrying multiple antibiotics provide enhanced synergistic effect and improved biocompatibility, Colloids Surf. B Biointerf. 175 (2019) 498–508, https://doi.org/10.1016/j.colsurfb.2018.12.035.
[118] S. Sachetelli, H. Khalil, T. Chen, C. Beaulac, S. Sénéchal, J. Lagacé, Demonstration of a fusion mechanism between a fluid bactericidal liposomal formulation and bacterial cells, Biochim. Biophys. Acta Biomembr. 1463 (2000) 254–266, https://doi.org/10.1016/S0005-2736(99)00217-5.
[119] C. Mugabe, M. Halwani, A.O. Azghani, R.M. Lafrenie, A. Omri, Mechanism of enhanced activity of liposome-entrapped aminoglycosides against resistant strains of *Pseudomonas aeruginosa*, Antimicrob. Agents Chemother. 50 (2006) 2016–2022, https://doi.org/10.1128/AAC.01547-05.
[120] N.D. Stebbins, M.A. Ouimet, K.E. Uhrich, Antibiotic-containing polymers for localized, sustained drug delivery, Adv. Drug Deliv. Rev. 78 (2014) 77–87, https://doi.org/10.1016/j.addr.2014.04.006.
[121] J. Kopeček, Polymer-drug conjugates: origins, progress to date and future directions, Adv. Drug Deliv. Rev. 65 (2013) 49–59, https://doi.org/10.1016/j.addr.2012.10.014.
[122] R.F.R.F. Landis, A. Gupta, Y.-W. Lee, L.-S. Wang, B. Golba, B. Couillaud, R. Ridolfo, R. Das, V.M.V.M. Rotello, Cross-linked polymer-stabilized nanocomposites for the treatment of bacterial biofilms, ACS Nano 11 (2016) 946–952, https://doi.org/10.1021/acsnano.6b07537.
[123] J. Cao, Y. Zhao, Y. Liu, S. Tian, C. Zheng, C. Liu, Y. Zhai, Y. An, H.J. Busscher, L. Shi, Y. Liu, Phosphorylcholine-based polymer encapsulated chitosan nanoparticles enhance the penetration of antimicrobials in a Staphylococcal biofilm, ACS Macro Lett. 8 (2019) 651–657, https://doi.org/10.1021/acsmacrolett.9b00142.
[124] P. Severino, M.V. Chaud, A. Shimojo, D. Antonini, M. Lancelloti, M.H.A. Santana, E.B. Souto, Sodium alginate-cross-linked polymyxin B sulphate-loaded solid lipid

nanoparticles: antibiotic resistance tests and HaCat and NIH/3T3 cell viability studies, Colloid. Surf. B Biointerf. 129 (2015) 191–197, https://doi.org/10.1016/j.colsurfb.2015.03.049.
[125] L.-L. Li, J.-H. Xu, G.-B. Qi, X. Zhao, F. Yu, H. Wang, Core–shell supramolecular gelatin nanoparticles for adaptive and "on-demand" antibiotic delivery, ACS Nano 8 (2014) 4975–4983, https://doi.org/10.1021/nn501040h.
[126] A.M. Mebert, C. Aimé, G.S. Alvarez, Y. Shi, S.A. Flor, S.E. Lucangioli, M. F. Desimone, T. Coradin, Silica core–shell particles for the dual delivery of gentamicin and rifamycin antibiotics, J. Mater. Chem. B 4 (2016) 3135–3144, https://doi.org/10.1039/C6TB00281A.
[127] W.L. Chiang, T.T. Lin, R. Sureshbabu, W.T. Chia, H.C. Hsiao, H.Y. Liu, C.M. Yang, H.W. Sung, A rapid drug release system with a NIR light-activated molecular switch for dual-modality photothermal/antibiotic treatments of subcutaneous abscesses, J. Control. Release 199 (2015) 53–62, https://doi.org/10.1016/j.jconrel.2014.12.011.
[128] J.M. Silva, E. Silva, R.L. Reis, Light-triggered release of photocaged therapeutics - where are we now? J. Control. Release 298 (2019) 154–176, https://doi.org/10.1016/j.jconrel.2019.02.006.
[129] B.J. Heilman, J.St. John, S.R.J. Oliver, P.K. Mascharak, Light-triggered eradication of *Acinetobacter baumannii* by means of NO delivery from a porous material with an entrapped metal nitrosyl, J. Am. Chem. Soc. 134 (2012) 11573–11582, https://doi.org/10.1021/ja3022736.
[130] A.Y. Rwei, W. Wang, D.S. Kohane, Photoresponsive nanoparticles for drug delivery, Nano Today 10 (2015) 451–467, https://doi.org/10.1016/j.nantod.2015.06.004.
[131] R. Weissleder, A clearer vision for in vivo imaging, Nat. Biotechnol. 19 (2001) 316–317, https://doi.org/10.1038/86684.
[132] Y. Chen, Y. Gao, Y. Chen, L. Liu, A. Mo, Q. Peng, Nanomaterials-based photothermal therapy and its potentials in antibacterial treatment, J. Control. Release 328 (2020) 251–262, https://doi.org/10.1016/j.jconrel.2020.08.055.
[133] D. Hu, H. Li, B. Wang, Z. Ye, W. Lei, F. Jia, Q. Jin, K.-F. Ren, J. Ji, Surface-adaptive gold nanoparticles with effective adherence and enhanced photothermal ablation of methicillin-resistant Staphylococcus aureus biofilm, ACS Nano 11 (2017) 9330–9339, https://doi.org/10.1021/acsnano.7b04731.
[134] D.G. Meeker, S.V. Jenkins, E.K. Miller, K.E. Beenken, A.J. Loughran, A. Powless, T.J. Muldoon, E.I. Galanzha, V.P. Zharov, M.S. Smeltzer, J. Chen, Synergistic photothermal and antibiotic killing of biofilm-associated Staphylococcus aureus using targeted antibiotic-loaded gold nanoconstructs, ACS Infect. Dis. 2 (2016) 241–250, https://doi.org/10.1021/acsinfecdis.5b00117.
[135] K.C.L. Black, T.S. Sileika, J. Yi, R. Zhang, J.G. Rivera, P.B. Messersmith, Bacterial killing by light-triggered release of silver from biomimetic metal nanorods, Small 10 (2014) 169–178, https://doi.org/10.1002/smll.201301283.
[136] Y. Zhao, X. Dai, X. Wei, Y. Yu, X. Chen, X. Zhang, C. Li, Near-infrared light-activated thermosensitive liposomes as efficient agents for photothermal and antibiotic synergistic therapy of bacterial biofilm, ACS Appl. Mater. Interfaces 10 (2018) 14426–14437, https://doi.org/10.1021/acsami.8b01327.
[137] B. Horev, M.I. Klein, G. Hwang, Y. Li, D. Kim, H. Koo, D.S.W. Benoit, pH-activated nanoparticles for controlled topical delivery of farnesol to disrupt oral biofilm virulence, ACS Nano 9 (2015) 2390–2404, https://doi.org/10.1021/nn507170s.
[138] K.R. Sims, Y. Liu, G. Hwang, H.I. Jung, H. Koo, D.S.W. Benoit, Enhanced design and formulation of nanoparticles for anti-biofilm drug delivery, Nanoscale 11 (2019) 219–236, https://doi.org/10.1039/c8nr05784b.
[139] L. Su, Y. Li, Y. Liu, R. Ma, Y. Liu, F. Huang, Y. An, Y. Ren, H.C. van der Mei, H. J. Busscher, L. Shi, Antifungal-inbuilt metal–organic-frameworks eradicate *Candida albicans* biofilms, Adv. Funct. Mater. 30 (2020) 2000537, https://doi.org/10.1002/adfm.202000537.
[140] J. Wu, F. Li, X. Hu, J. Lu, X. Sun, J. Gao, D. Ling, Responsive assembly of silver nanoclusters with a biofilm locally amplified bactericidal effect to enhance treatments against multi-drug-resistant bacterial infections, ACS Cent. Sci. 5 (2019) 1366–1376, https://doi.org/10.1021/acscentsci.9b00359.
[141] Y. Gao, J. Wang, M. Chai, X. Li, Y. Deng, Q. Jin, J. Ji, Size and charge adaptive clustered nanoparticles targeting the biofilm microenvironment for chronic lung infection management, ACS Nano 14 (2020) 5686–5699, https://doi.org/10.1021/acsnano.0c00269.
[142] S. Yang, X. Han, Y. Yang, H. Qiao, Z. Yu, Y. Liu, J. Wang, T. Tang, Bacteria-targeting nanoparticles with microenvironment-responsive antibiotic release to eliminate intracellular *Staphylococcus aureus* and associated infection, ACS Appl. Mater. Interfaces 10 (2018) 14299–14311, https://doi.org/10.1021/acsami.7b15678.
[143] H. Singh, W. Li, M.R. Kazemian, R. Yang, C. Yang, S. Logsetty, S. Liu, Lipase-responsive electrospun theranostic wound dressing for simultaneous recognition and treatment of wound infection, ACS Appl. Bio Mater. 2 (2019) 2028–2036, https://doi.org/10.1021/acsabm.9b00076.
[144] D. Yang, X. Lv, L. Xue, N. Yang, Y. Hu, L. Weng, N. Fu, L. Wang, X. Dong, A lipase-responsive antifungal nanoplatform for synergistic photodynamic/photothermal/pharmaco-therapy of azole-resistant: *Candida albicans* infections, Chem. Commun. 55 (2019) 15145–15148, https://doi.org/10.1039/c9cc08463k.
[145] M.H. Xiong, Y. Bao, X.Z. Yang, Y.C. Wang, B. Sun, J. Wang, Lipase-sensitive polymeric triple-layered nanogel for "on-demand" drug delivery, J. Am. Chem. Soc. 134 (2012) 4355–4362, https://doi.org/10.1021/ja211279u.
[146] Y. Li, G. Liu, X. Wang, J. Hu, S. Liu, Enzyme-responsive polymeric vesicles for bacterial-strain-selective delivery of antimicrobial agents, Angew. Chem. Int. Ed. 55 (2016) 1760–1764, https://doi.org/10.1002/anie.201509401.
[147] M.-H. Xiong, Y.-J. Li, Y. Bao, X.-Z. Yang, B. Hu, J. Wang, Bacteria-responsive multifunctional nanogel for targeted antibiotic delivery, Adv. Mater. 24 (2012) 6175–6180, https://doi.org/10.1002/adma.201202847.
[148] Y. Zhang, P. Sun, L. Zhang, Z. Wang, F. Wang, K. Dong, Z. Liu, J. Ren, X. Qu, Silver-infused porphyrinic metal–organic framework: surface-adaptive, on-demand nanoplatform for synergistic bacteria killing and wound disinfection, Adv. Funct. Mater. 29 (2019) 1808594, https://doi.org/10.1002/adfm.201808594.
[149] S. Haas, N. Hain, M. Raoufi, S. Handschuh-Wang, T. Wang, X. Jiang, H. Schönherr, Enzyme degradable polymersomes from hyaluronic acid-block-poly (ε-caprolactone) copolymers for the detection of enzymes of pathogenic bacteria, Biomacromolecules 16 (2015) 832–841, https://doi.org/10.1021/bm501729h.
[150] M. Chen, S. Xie, J. Wei, X. Song, Z. Ding, X. Li, Antibacterial micelles with vancomycin-mediated targeting and pH/lipase-triggered release of antibiotics, ACS Appl. Mater. Interfaces 10 (2018) 36814–36823, https://doi.org/10.1021/acsami.8b16092.
[151] Y. Su, L. Zhao, F. Meng, Z. Qiao, Y. Yao, J. Luo, Triclosan loaded polyurethane micelles with pH and lipase sensitive properties for antibacterial applications and treatment of biofilms, Mater. Sci. Eng. C 93 (2018) 921–930, https://doi.org/10.1016/j.msec.2018.08.063.
[152] D. Pornpattananangkul, L. Zhang, S. Olson, S. Aryal, M. Obonyo, K. Vecchio, C.-M. Huang, L. Zhang, Bacterial toxin-triggered drug release from gold nanoparticle-stabilized liposomes for the treatment of bacterial infection, J. Am. Chem. Soc. 133 (2011) 4132–4139, https://doi.org/10.1021/ja111110e.
[153] C.Y. Zhang, J. Gao, Z. Wang, Bioresponsive nanoparticles targeted to infectious microenvironments for sepsis management, Adv. Mater. 30 (2018) 1803618, https://doi.org/10.1002/adma.201803618.
[154] M. Xiong, Y. Bao, X. Xu, H. Wang, Z. Han, Z. Wang, Y. Liu, S. Huang, Z. Song, J. Chen, R.M. Peek Jr., L. Yin, L.-F. Chen, J. Cheng, Selective killing of *Helicobacter pylori* with pH-responsive helix-coil conformation transitionable antimicrobial polypeptides, Proc. Natl. Acad. Sci. U. S. A. 114 (2017) 12675–12680, https://doi.org/10.1073/pnas.1710408114.
[155] M. Xiong, Z. Han, Z. Song, J. Yu, H. Ying, L. Yin, J. Cheng, Bacteria-assisted activation of antimicrobial polypeptides by a random-coil to helix transition, Angew. Chem. Int. Ed. 56 (2017) 10826–10829, https://doi.org/10.1002/anie.201706071.
[156] H. Ji, K. Dong, Z. Yan, C. Ding, Z. Chen, J. Ren, X. Qu, Bacterial hyaluronidase self-triggered prodrug release for chemo-photothermal synergistic treatment of bacterial infection, Small 12 (2016) 6200–6206, https://doi.org/10.1002/smll.201601729.
[157] Y. Li, Y. Liu, R. Ma, Y. Xu, Y. Zhang, B. Li, Y. An, L. Shi, A G-quadruplex hydrogel via multicomponent self-assembly: formation and zero-order controlled release, ACS Appl. Mater. Interfaces 9 (2017) 13056–13067, https://doi.org/10.1021/acsami.7b00957.
[158] Z. Chen, Z. Wang, J. Ren, X. Qu, Enzyme mimicry for combating bacteria and biofilms, Acc. Chem. Res. 51 (2018) 789–799, https://doi.org/10.1021/acs.accounts.8b00011.
[159] H. Shi, Y. Liu, R. Qu, Y. Li, R. Ma, Y. An, L. Shi, A facile one-pot method to prepare peroxidase-like nanogel artificial enzymes for highly efficient and controllable catalysis, Colloids Surf. B Biointerf. 174 (2019) 352–359, https://doi.org/10.1016/j.colsurfb.2018.11.021.
[160] C.-H. Yu, G.-Y. Chen, M.-Y. Xia, Y. Xie, Y.-Q. Chi, Z.-Y. He, C.-L. Zhang, T. Zhang, Q.-M. Chen, Q. Peng, Understanding the sheet size-antibacterial activity relationship of graphene oxide and the nano-bio interaction-based physical mechanisms, Colloids Surf. B Biointerf. 191 (2020) 111009, https://doi.org/10.1016/j.colsurfb.2020.111009.
[161] M.-Y. Xia, Y. Xie, C.-H. Yu, G.-Y. Chen, Y.-H. Li, T. Zhang, Q. Peng, Graphene-based nanomaterials: the promising active agents for antibiotics-independent antibacterial applications, J. Control. Release 307 (2019) 16–31, https://doi.org/10.1016/j.jconrel.2019.06.011.